12-2011

The Performance of Serial, Matched-Filter Packet Acquisition Using Transmit and Receive Antenna Diversity

Shivram Ramanathan
Clemson University, sramana@clemson.edu

The Performance of Serial, Matched-Filter Packet Acquisition Using Transmit and Receive Antenna Diversity

---

A Dissertation
Presented to
the Graduate School of
Clemson University

In Partial Fulfillment
of the Requirements for the Degree
Master of Science
Electrical Engineering

---

by
Shivram Ramanathan
December 2011

Accepted by:
Dr. Daniel L. Noneaker, Committee Chair
Dr. Michael B. Pursley
Dr. Harlan B. Russell

Abstract

The performance of serial, matched-filter acquisition is evaluated for asynchronous packet radio communications using transmit or receive antenna diversity. Transmit diversity is achieved using dual antenna transmissions of orthogonal preamble sequences and receive diversity is achieved using dual antenna reception of a single preamble sequence. Sequential test statistics are formed using non-coherent combining of the outputs from the orthogonal preamble matched-filters if transmitter diversity is used; the test statistics are formed using non coherent combining of the outputs from the preamble matched-filter in each receiver chain if receiver diversity is used. Threshold-based acquisition of the test statistics using both fixed and adaptive acquisition thresholds is considered. The effect of the intermediate-frequency filter and the automatic gain control subsystem on the acquisition performance is accounted for. The performance is evaluated in additive white Gaussian noise channels with constant and slowly varying gains (i.e., a slow-fading channel). The effect of fixed and adaptive acquisition thresholds on the link outage probability is compared for each dual antenna diversity acquisition system. The acquisition performance using transmit or receive antenna diversity is compared with the performance of a system lacking antenna diversity, for both fixed and adaptive threshold acquisition.

Dedication

To Amma, Appa, Karthik, the rest of my family and all the teachers who have taught and guided me over the years.

Acknowledgments

I am extremely grateful to Prof. Noneaker for guiding me through every step of this thesis patiently, and supporting me in all my endeavors. I would also like to thank Prof. Pursley and Prof. Russell for their invaluable inputs and the great classes that they taught.

I am thankful to the CommNet research group in the Electrical and Computer Engineering Department at Clemson which provided me a friendly and conducive environment to do my research. I would like to thank all my friends who made sure I enjoyed my life outside of work. Last but not the least, this work would have been impossible without the Satsanga at Clemson, who gave me the inspiration to better myself.

Table of Contents

List of Figures

Chapter 1

Introduction

An unslotted packet radio communication network is designed to permit each radio node to transmit at a time that is not constrained to a discrete set of predetermined times. Successful demodulation of the packet's data by the receiver requires that the receiver detect the arrival of the packet transmission and identify the start of the data content. This is often implemented by including a preamble sequence at the start of every packet transmission, where the sequence is known *a priori* at the receiver. There is *a priori* uncertainty about the time of arrival of the preamble at the receiver, however. This uncertainty is resolved and an initial alignment of chip or symbol timing to a local reference is provided in the acquisition stage. A subsequent tracking stage then maintains synchronism throughout the reception of the packet using a delay-locked loop [1] or a similar circuit. The receiver's ability to acquire a packet can be the limiting factor in the performance of the radio link.

A serial matched-filter acquisition technique is considered in this thesis in which test statistics are derived from sampled matched-filter outputs and compared sequentially against an acquisition threshold [2]. In previous work, the performance of non-coherent, serial, matched-filter acquisition with a fixed acquisition threshold is evaluated for an additive white Gaussian noise (AWGN) channel [3]. It is shown that the probability of not acquiring is a non-monotonic function of the signal-to-noise ratio at the receiver, due to the effect of the intermediate-frequency (IF) filter and the automatic gain control (AGC)

subsystem in the down conversion chain of the heterodyne receiver. By using the threshold-adaptation algorithm proposed in [4], the severity of this non-monotonicity can be reduced substantially, thus resulting in significant improvement in the acquisition performance over fixed threshold acquisition in an AWGN channel.

In mobile communications, however, the presence of slow channel fading results in outages during which the system does not meet its target performance for an extended period of time. In these instances, the use of multiple transmitting or receiving antennas with sufficient spatial or polarization separation can help provide diversity and mitigate the effect of fading, resulting in less frequent outages. For example, dual transmission antennas can be combined with appropriate space-time coding to yield diversity protection against fading without sacrificing spectral efficiency during the data portion of a packet transmission [5]. Alternatively, the signal from a single transmitting antenna can be received on two separate receivers with appropriate techniques for combining the outputs of the two receiver chains, which doubles the signal power received over equal-gain channels as well as provides diversity protection against fading [6]. A combination of transmit and receive antenna diversity can also be used to reap the benefits of both. The presence of channel fading and the use of transmit and receive antenna diversity introduce new considerations to the design and performance of the fixed-threshold and adaptive-threshold acquisition algorithms presented in [3] and [4]. The effect of the diversity techniques on the system's acquisition performance is considered in this thesis.

Three systems are considered in the thesis. The first system consists of a transmitting radio with a single antenna and a receiving radio with a single antenna. The system is highly susceptible to periods of severe attenuation (fading) of the radio-frequency (RF) signal.

The second system consists of a transmitting radio with two antennas and a receiving radio with a single antenna. The two transmitting antennas emit orthogonal RF signals so that they can be separated at the receiver. The signals from the two antennas undergo fading with a low correlation if the transmitting antennas are spaced sufficiently far apart.

The resulting transmission diversity [5] ensures that a strong signal is received from at least one of the transmitting antennas with a high probability.

The third system consists of a transmitting radio with a single antenna and a receiving radio with two antennas. The transmitted signal to the two receivers undergoes fading with a low correlation if the receiving antennas are spaced sufficiently far apart. As a result of the receiver diversity, there is a strong signal received in at least one of the receiving antennas with a high probability.

The thesis is organized as follows. The transmitters, channels, receivers and the acquisition algorithms used for the three systems mentioned above are described in detail in Chapter 2. In Chapter 3, the performance of the single-transmitter, single-receiver system is evaluated using both analytical techniques and simulation for communications in both an AWGN channel with constant attenuation and an AWGN channel with time-varying attenuation (i.e., a fading channel). Similarly, the performance for the dual-transmitter, single-receiver system and the single-transmitter, dual-receiver system is evaluated in Chapters 4 and 5, respectively; it is compared with the performance of the single-transmitter, single-receiver system in both constant and time-varying AWGN channels. Conclusions are given in Chapter 6.

Chapter 2

System Description

The transmission format, channel, receiver architecture, and acquisition algorithms are defined in this chapter for each of the three systems considered in the thesis.

2.1 Transmitted Signals

2.1.1 Single-Transmitter System

The transmitted RF signal for the system using a single transmitting antenna is given by

$$s(t) = \mathrm{Re}\{\tilde{s}(t)e^{j2\pi f_c t}\}$$

where f_c is the frequency of the RF carrier. It consists of an M-chip preamble followed by the data content of the packet. The baseband-equivalent preamble is given by

$$\tilde{s}(t) = \sqrt{P}\, c(t)\, p_{MT_c}(t)$$

where P is the transmission power used for the preamble section of the signal, T_c is the chip duration of the waveform, and $p_T(t)$ is the unit amplitude rectangular pulse over $[0, T)$.

The quaternary phase-shift-keyed preamble waveform is given by

$$c(t) = \sum_{i=0}^{M-1} a_i \psi(t - iT_c)$$

where $\{a_i\}$ is a complex-valued quaternary preamble sequence of chips which can take values from $\{e^{j(\pi/4)}, e^{j(3\pi/4)}, e^{j(5\pi/4)}, e^{j(7\pi/4)}\}$. The unit-power chip waveform $\psi(t)$ is time-limited to $[0, T_c)$.

2.1.2 Dual-Transmitter System

The two transmitting antennas in the dual-transmitter system are denoted by antenna zero and antenna one, and they transmit concurrently. The transmitted RF signal at transmitting antenna l for the system using dual transmitting antennas is given by

$$s_l(t) = \mathrm{Re}\{\tilde{s}_l(t) e^{j2\pi f_c t}\},\ 0 \le l \le 1\ ,$$

where the same RF carrier frequency f_c is used at both transmitting antennas. Orthogonal preamble sequences $\{a_{0,i}\}$ and $\{a_{1,i}\}$ of M chips each are used by transmitting antennas zero and one, respectively. The two preamble sequences are constructed from a single quaternary sequence $\{a_i\}$ using the technique described in [5]. The baseband-equivalent preamble signal at transmitting antenna l is given by

$$\tilde{s}_l(t) = \sqrt{\frac{P}{2}}\, c_l(t)\, p_{MT_c}(t)$$

where

$$c_l(t) = \sum_{i=0}^{M-1} a_{l,i} \psi(t - iT_c),\ 0 \le l \le 1\ .$$

Transmitting antennas zero and one transmit their respective preamble signals with transmit power $P/2$ so that the total preamble power transmitted by the two antennas is P.

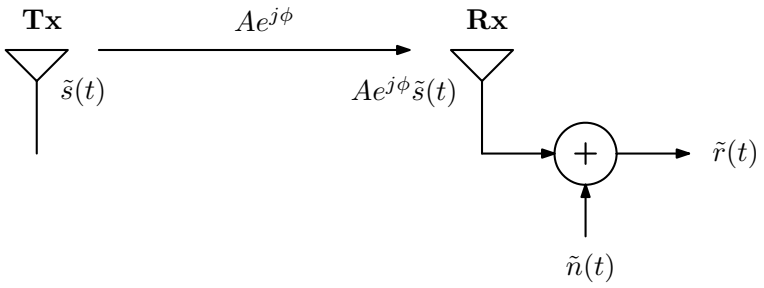

Figure 2.1: Baseband-equivalent single-transmitter, single-receiver system.

2.2 Channels and Received Signals

The channel between each transmitting antenna and a receiving antenna consists of a single propagation path that introduces a magnitude change and a phase shift of the RF signal. The magnitude change and phase shift may vary between consecutive packet transmissions. They are constant over the duration of each preamble, however; thus, the channel exhibits non-selective fading over each preamble. The signal is distorted by AWGN at the front-end of the receiver.

2.2.1 Single-Transmitter, Single-Receiver System

The transmitted preamble arrives at the receiver over a channel with channel gain A and a phase offset ϕ. The received RF signal is thus given by

$$r(t) = \mathrm{Re}\{\tilde{r}(t)e^{j2\pi f_c t}\}$$

where the baseband-equivalent received signal is given by

$$\tilde{r}(t) = A\ e^{j\phi}\ \tilde{s}(t) + \tilde{n}(t).$$

The complex-valued, baseband-equivalent AWGN process $\tilde{n}(t)$ has a two-sided power spectral density of N_0. This scenario is illustrated in Fig. 2.1. The *instantaneous preamble*

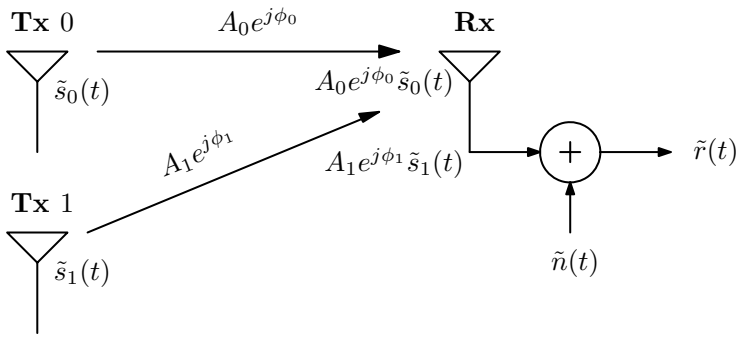

Figure 2.2: Baseband-equivalent dual-transmitter, single-receiver system.

signal-to-noise ratio, SNR, at the receiver is

$$SNR = A^2 \frac{MPT_C}{N_0}.$$

We consider a channel that exhibits Rician fading [7]. That is, the random variable A has a Rician distribution, ϕ is uniformly distributed over $[0, 2\pi)$, and A and ϕ are independent. The channel's fading is thus determined by two parameters:

$$\mathrm{E}[A] = \mu \ \text{ and } \ \mathrm{Var}(A) = 2\sigma^2.$$

The *specular-to-diffuse energy ratio* ($SDER$) of the channel is given by $\mu^2/2\sigma^2$, and the *average signal-to-noise ratio* at the receiver is given by

$$\overline{SNR} = \mathrm{E}_A[SNR] = (\mu^2 + 2\sigma^2)\frac{MPT_c}{N_0}. \tag{2.1}$$

If $\sigma = 0$, the channel is non-fading; if instead $\mu = 0$, it is a Rayleigh-fading channel.

2.2.2 Dual-Transmitter, Single-Receiver System

The transmitted packet from transmitting antenna l arrives at the receiver over a channel with gain A_l and a phase offset ϕ_l, for $l = 0, 1$, as shown in Fig. 2.2. The received

RF signal is thus given by

$$r(t) = \mathrm{Re}\{\tilde{r}(t)e^{j2\pi f_c t}\}$$

where the baseband-equivalent received signal is given by

$$\tilde{r}(t) = A_0\, e^{j\phi_0}\, \tilde{s}_0(t) + A_1\, e^{j\phi_1}\, \tilde{s}_1(t) + \tilde{n}(t).$$

The complex-valued, baseband-equivalent AWGN process $\tilde{n}(t)$ has a two-sided power spectral density of N_0. The instantaneous preamble signal-to-noise ratio at the receiver is given by

$$SNR = \left(\frac{A_0^2 + A_1^2}{2}\right)\frac{MPT_C}{N_0}. \tag{2.2}$$

The channels from the two transmitting antennas to the receiver exhibit identically distributed Rician fading with

$$\mathrm{E}[A_l] = \mu \ \text{ and } \ \mathrm{Var}(A_l) = 2\sigma^2.$$

The specular-to-diffuse energy ratio of each channel is thus $\mu^2/2\sigma^2$, and the average signal-to-noise ratio at the receiver is given by equation (2.1). We consider the circumstance in which the transmitting antennas are spaced far enough apart that the two channels exhibit independent fading; thus, A_0,A_1,ϕ_0 and ϕ_1 are mutually independent random variables.

2.2.3 Single-Transmitter, Dual-Receiver System

The transmitted packet arrives at receiving antenna l over a channel with gain A_l and a phase offset ϕ_l, for $l = 0, 1$, as shown in Fig. 2.3. The RF signal at receiving antenna l is thus given by

$$r_l(t) = \mathrm{Re}\{\tilde{r}_l(t)e^{j2\pi f_c t}\}$$

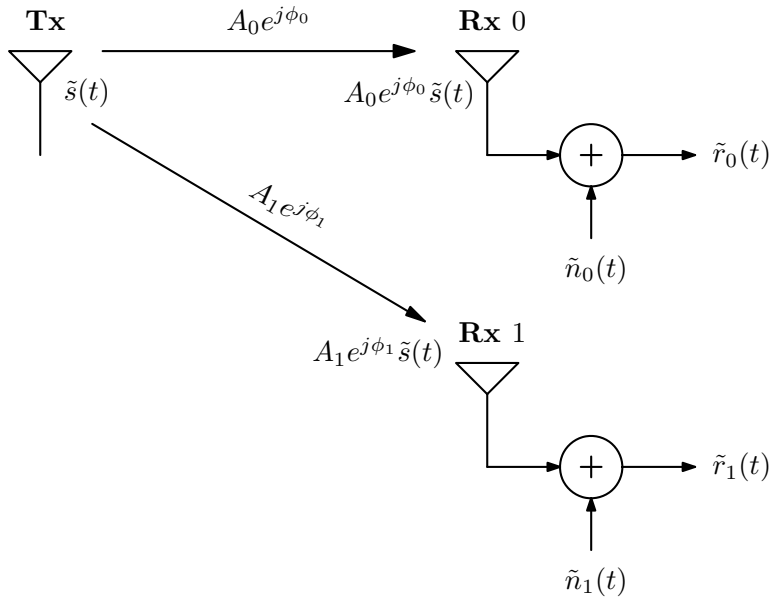

Figure 2.3: Baseband-equivalent single-transmitter, dual-receiver system.

where the baseband-equivalent signal at receiver l is

$$\tilde{r}_l(t) = A_l \, e^{j\phi_l} \, \tilde{s}(t) + \tilde{n}_l(t).$$

The complex-valued, baseband-equivalent AWGN process $\tilde{n}_l(t)$ has two-sided power spectral density N_l, for $l = 0, 1$. The noise processes at the two antennas are independent, and they need not have the same power spectral density in general.

Without loss of generality, we assume that $N_0 \leq N_1$. The noise power spectral density at receiving antenna zero is viewed as the nominal value; thus, the circumstance in which $N_1 > N_0$ is viewed as one in which the RF front end of the receiver chain for antenna one contains degraded electronics resulting in a noise figure [8] below the nominal value. We define the *noise-factor degradation* at receiver antenna one as

$$\gamma = \frac{N_1}{N_0},$$

or equivalently,

$$\gamma_{dB} = 10 \log_{10} \left(\frac{N_1}{N_0} \right) (\text{dB}).$$

Comparisons of the performance between the single-receiver systems and the dual-receiver system requires a measure that fairly reflects the cost in transmitted power for all the systems. The *instantaneous signal-to-noise ratio* is thus given by,

$$SNR = \frac{1}{2} \left(A_0^2 + \gamma^{-1} A_1^2 \right) \frac{MPT_c}{N_0}. \tag{2.3}$$

It is the signal-to-noise ratio achieved at the receiver by maximal-ratio combining [6] of the two received signals, with a factor of $1/2$ to account for a fair comparison of the single-receiver systems with the dual-receiver system in the case in which its two receiver chains have identical RF and IF components. For comparing the performance of the single-transmitter, dual-receiver system under different values of γ we define the *nominal instantaneous received signal-to-noise ratio*,

$$SNR_{nom} = SNR|_{\gamma=1} = \left(\frac{A_0^2 + A_1^2}{2} \right) \frac{MPT_c}{N_0}.$$

The channels from the transmitting antenna to the two receiving antennas exhibit identically distributed Rician fading, with

$$\mathrm{E}[A_l] = \mu \ \text{ and } \ \mathrm{Var}(A_l) = 2\sigma^2.$$

The specular-to-diffuse energy ratio of each channel is thus $\mu^2/2\sigma^2$, and the average signal-to-noise ratio is given by

$$\overline{SNR} = (\mu^2 + 2\sigma^2) \left(1 + \gamma^{-1} \right) \frac{MPT_c}{2N_0}. \tag{2.4}$$

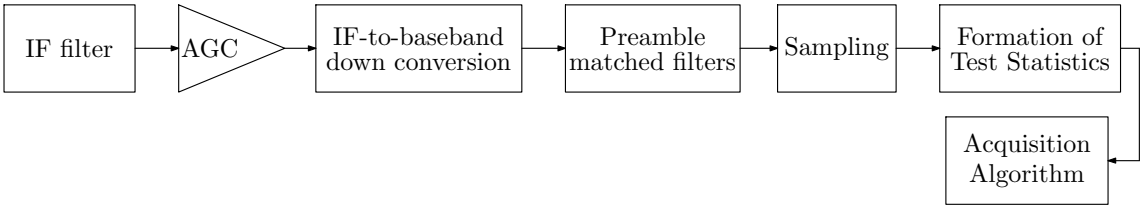

Figure 2.4: The single-antenna receiver chain for matched-filter packet acquisition.

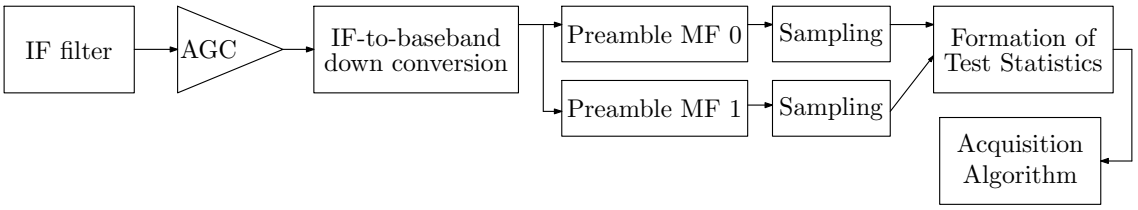

Figure 2.5: The single-antenna receiver chain for matched-filter packet acquisition with two transmitting antennas.

The average nominal signal-to-noise ratio at the receiver is given by

$$\overline{SNR}_{nom} = (\mu^2 + 2\sigma^2)\frac{MPT_c}{N_0}.$$

We consider the circumstance in which the receiving antennas are spaced far enough apart that the two channels exhibit independent fading.

2.3 Receiver Architecture

The receivers for the single-receiver and dual-receiver systems are built from the same functional blocks. The single-receiver system has one receiver chain. The receiver chain is a heterodyne receiver [8], and the effect of its first stage (RF-to-IF conversion) on the received signal is assumed to result in no distortion of the signal. The IF signal is thus given by

$$r_{IF}(t) = \mathrm{Re}\{\tilde{r}(t)e^{j2\pi f_{IF}t}\} \tag{2.5}$$

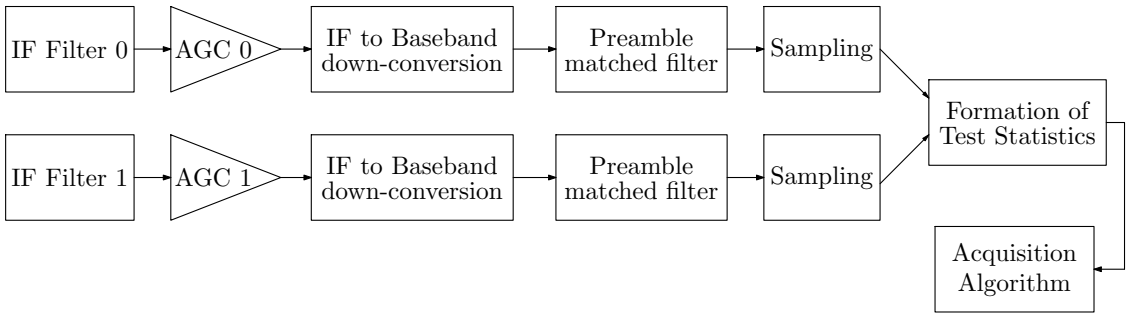

Figure 2.6: The two-antenna receiver chain for matched-filter packet acquisition.

where f_{IF} is the intermediate frequency in hertz.

The portion of the receiver after the RF-to-IF downconverter can be modeled approximately by the following functional blocks in series (as shown in Fig. 2.4): the IF bandpass filter, the AGC subsystem, I-Q demodulation to baseband, preamble-matched filtering, sampling and signal processing to form the test statistics [4]. The dual-transmitter system's receiver shown in Fig. 2.5 is identical to the one given by Fig. 2.4 except that the baseband downconverted AGC output is passed in parallel to filters matched to each of the orthogonal preamble sequences and the two matched filter outputs are used in the formation of test statistics. The statistics are then passed sequentially to a serial acquisition algorithm. The bandwidth of the IF filter is assumed to be large enough that it does not introduce distortion into the signal component of the received IF signal (although its bandwidth does affect the total signal-plus-noise power into the AGC subsystem).

The dual-receiver system employs a separate receiver chain for each antenna's output with the IF signal given by

$$r_{IF,l}(t) = \mathrm{Re}\{\tilde{r}_l(t)e^{j2\pi f_{IF}t}\} \tag{2.6}$$

in the receiver chain for receiving antenna l, for $l = 0, 1$. The concurrent output of the two chains at any sampling time are used to form a single test statistic, as shown in Fig. 2.6. Each functional block in the receiver is described below for each of the three systems, highlighting the differences among the systems.

2.3.1 Single-Transmitter, Single-Receiver System

The received signal in equation (2.5) is passed through an IF filter with baseband-equivalent impulse response $\tilde{h}(t)$. Without loss of generality, it is assumed that

$$\max_f \mid \tilde{H}(f) \mid = 1$$

where $\tilde{H}(f)$ is the baseband-equivalent frequency response of the filter. The output of the IF filter is passed through an AGC subsystem with time-varying power gain $\alpha(t)$. The AGC subsystem considered is one which responds instantly to step changes in the input power and maintains a constant average output power [3]. The baseband-equivalent output of the AGC subsystem is

$$\hat{r}(t) = \sqrt{\alpha(t)}(\tilde{r} * \tilde{h})(t) = Ae^{j\phi}\hat{s}(t) + \hat{n}(t) \tag{2.7}$$

where "'$*$" is the convolution operator,

$$\hat{s}(t) = \sqrt{\alpha(t)}(\tilde{s} * \tilde{h})(t),$$
$$\hat{n}(t) = \sqrt{\alpha(t)}(\tilde{n} * \tilde{h})(t)$$

and

$$\alpha(t) = \begin{cases} \alpha_0 & = G\left(\frac{\gamma_s \beta N_0}{T_c}\right)^{-1}, & \mathrm{t} < 0, \\ \alpha_1 & = G\gamma_s^{-1}\left(A^2 P + \frac{\beta N_0}{T_c}\right)^{-1}, & 0 \leq \mathrm{t} \leq \mathrm{MT_c} \end{cases}. \tag{2.8}$$

The parameter G equals the average AGC output power, and the other parameters in equation (2.8) are given by

$$\gamma_s = \int_{-\infty}^{\infty} \frac{|\Psi(f)|^2}{T_c} |\tilde{H}(f)|^2 df, \tag{2.9}$$
$$\gamma_n = T_c \int_{-\infty}^{\infty} |\tilde{H}(f)|^2 df, \tag{2.10}$$

and

$$\beta = \gamma_n/\gamma_s \tag{2.11}$$

where $\Psi(f)$ is the Fourier transform of the chip waveform. The IF signal at the AGC output is passed through an I-Q demodulator and the demodulator's complex-valued output is the input to a filter $g(t)$ matched to the transmitted preamble signal $c(t)$. The matched filter is thus given by

$$g(t) = \sum_{i=0}^{M-1} a^*_{M-1-i}\psi(t - iT_c). \tag{2.12}$$

The complex-valued output of the filter sampled at time t is denoted by $Z(t)$. It is used to form the square-law decision statistic $X(t) =\mid Z(t) \mid^2$, which is provided as an input to the acquisition algorithm.

2.3.2 Dual-Transmitter, Single-Receiver System

The received signal in equation (2.5) is passed through an IF filter and an AGC subsystem with the same respective characteristics as in the single-transmitter, single-receiver system. The baseband-equivalent output of the AGC subsystem is thus

$$\hat{r}(t) = \sqrt{\alpha(t)}(\tilde{r} * \tilde{h})(t) = A_0 e^{j\phi_0}\hat{s}_0(t) + A_1 e^{j\phi_1}\hat{s}_1(t) + \hat{n}(t) \tag{2.13}$$

where

$$\begin{aligned}
\hat{s}_l(t) &= \sqrt{\alpha(t)}(\tilde{s}_l * \tilde{h})(t),\ 0 \le l \le 1, \\
\hat{n}(t) &= \sqrt{\alpha(t)}(\tilde{n} * \tilde{h})(t)
\end{aligned}$$

and

$$\alpha(t) = \begin{cases} \alpha_0 & = G\left(\frac{\gamma_s \beta N_0}{T_c}\right)^{-1}, & \mathrm{t} < 0, \\ \alpha_1 & = G\gamma_s^{-1}\left(\left(\frac{A_0^2 + A_1^2}{2}\right)P + \frac{\beta N_0}{T_c}\right)^{-1}, & 0 \le \mathrm{t} \le \mathrm{MT_c} \end{cases}. \tag{2.14}$$

The parameters in equation (2.14) are given by equations (2.9)-(2.11). The IF signal at the AGC output is passed through an I-Q demodulator and the demodulator's complex-valued output is provided in parallel to filters $g_0(t)$ and $g_1(t)$ which are matched to the orthogonal transmitted preamble signals $c_0(t)$ and $c_1(t)$, respectively. The matched filters are thus given by

$$g_l(t) = \sum_{i=0}^{M-1} a^*_{l,M-1-i}\psi(t - iT_c),\ 0 \leq l \leq 1. \tag{2.15}$$

The complex-valued outputs of the two matched-filters sampled at time t are denoted by $Z_0(t)$ and $Z_1(t)$. They are used to form the square-law decision statistic,

$$X(t) = |Z_0(t)|^2 + |Z_1(t)|^2,$$

which is provided as an input to the acquisition algorithm.

2.3.3 Single-Transmitter, Dual-Receiver System

The received signal $r_l(t)$ in equation (2.6) is passed through an IF filter with the baseband-equivalent impulse response $\tilde{h}_l(t)$, for $l = 0, 1$. Without loss of generality, it is assumed that

$$\max_f \mid \tilde{H}_l(f) \mid = 1,$$

where $\tilde{H}_l(f)$ is the baseband-equivalent frequency response of the filter in receiver chain l. The IF filter output in receiver chain l is passed through an AGC subsystem with the same characteristics as the AGC system in the single-receiver systems. The baseband-equivalent output of the AGC subsystem in receiver chain l is thus given by

$$\hat{r}_l(t) = \sqrt{\alpha_l(t)}(\tilde{r}_l * \tilde{h}_l)(t) = A_l e^{j\phi_l}\hat{s}_l(t) + \hat{n}_l(t) \tag{2.16}$$

where

$$\hat{s}_l(t) = \sqrt{\alpha_l(t)}(\tilde{s} * \tilde{h}_l)(t),$$

$$\hat{n}_l(t) = \sqrt{\alpha_l(t)}(\tilde{n}_l * \tilde{h}_l)(t)$$

and

$$\alpha_l(t) = \begin{cases} \alpha_{l,0} & = G_l \left(\frac{\gamma_s \beta_l N_l}{T_c}\right)^{-1}, & \text{t} < 0, \\ \alpha_{l,1} & = G_l \gamma_s^{-1} \left(A_l^2 \tilde{P} + \frac{\beta_l N_l}{T_c}\right)^{-1}, & 0 \leq \text{t} \leq \text{MT}_\text{c} \end{cases} \tag{2.17}$$

for $l = 0, 1$. The average output power of the AGC subsystem in receiver chain l is thus G_l, and the other parameters in equation (2.17) are given by

$$\gamma_{s,l} = \int_{-\infty}^{\infty} \frac{|\Psi(f)|^2}{T_c} |\tilde{H}_l(f)|^2 df, \tag{2.18}$$

$$\gamma_{n,l} = T_c \int_{-\infty}^{\infty} |\tilde{H}_l(f)|^2 df, \tag{2.19}$$

and

$$\beta_l = \gamma_{n,l}/\gamma_{s,l}. \tag{2.20}$$

The IF signal at the AGC output in each receiver chain is passed through an I-Q demodulator. The complex-valued output of each demodulator is the input to a filter with the impulse response $g(t)$ given by equation (2.12). The complex-valued outputs of the filter in receiver chains zero and one sampled at time t are denoted by $Z_0(t)$ and $Z_1(t)$, respectively. They are used to form the square-law decision statistic,

$$X(t) = |Z_0(t)|^2 + |Z_1(t)|^2,$$

which is provided as the input to the acquisition algorithm.

2.4 Acquisition Algorithm

For each of the three systems addressed in this thesis, two serial acquisition algorithms are considered: a fixed-threshold algorithm [3] and an adaptive-threshold algorithm [4]. A practical acquisition system employs a sampling rate at the matched-filter out-

put(s) that is two to four times the chip rate, since the chip timing is unknown *a priori* at the receiver. The performance of the over-sampling acquisition algorithm is approximated with reasonable accuracy by an algorithm that employs one sample per chip and an optimal sampling time [1]. The approximation of chip-rate, chip-synchronous sampling of the matched-filter output is used in this thesis. A test statistic $X_k = X(kT_c)$ is thus provided as input to the acquisition algorithm once per chip interval.

The receiver is nominally in the *acquisition mode* in which it monitors the channel for the arrival of a packet transmission. If the receiver detects the apparent arrival of the complete preamble of a packet with a given time of arrival, it enters the *verification mode*. While it is in verification mode, the receiver performs additional processing to determine with a high probability whether an arrival has indeed occurred at the apparent time of arrival. If the packet arrival is not verified, the receiver returns to the acquisition mode. If a packet arrival is verified, the receiver enters the *data-detection mode* during which it detects the data content of the packet. Afterwards, it returns to the acquisition mode.

A threshold-based serial acquisition algorithm is used during the acquisition mode. The test statistics are considered sequentially, and each test statistic X_k is compared against a threshold η_k (which differs in general for different k). If $X_k > \eta_k$, a *hit* is declared at time $t = kT_c$ and the receiver enters the verification mode. No hits are declared while the receiver is in the verification mode, and the corresponding test statistics are ignored. A hit that occurs at a time other than the correct time (i.e., other than at time $t = MT_c$) is referred to as a *false alarm*.

Three outcomes are possible when a packet is transmitted on a previously idle channel. If no recent false alarms have occurred so that the receiver is in the acquisition mode at time $t = MT_c$, the statistic X_M is tested in the acquisition algorithm. If a hit occurs, the verification mode is entered. Otherwise, a *miss* occurs, the receiver remains in the acquisition mode and it fails to acquire the packet. Alternatively, the receiver may be in the verification mode at time $t = MT_c$ due to a recent false alarm so that the acquisition mode is inactive; the receiver also fails to acquire the packet in this instance.

A properly designed verification mode can correctly classify a hit as valid or invalid with a high probability. We thus assume that the verification mode always correctly identifies the occurrence of an arrival. Consequently, a hit at time $t = MT_c$ results in successful packet acquisition (whereas either a false alarm or a miss results in a failure to acquire the packet). In this thesis, we consider an arbitrary fixed-length *verification interval* of duration QT_c for each instance of acquisition verification. The *probability of not acquiring* is thus given by

$$P_{nacq} = 1 - \Pr\left(\bigcap_{k=M-Q}^{M-1} \{X_k < \eta_k\} \bigcap \{X_M > \eta_M\}\right).$$

2.4.1 Fixed-Threshold Acquisition Algorithm

The fixed threshold acquisition algorithm uses a constant predetermined threshold η. That is, $\eta_k = \eta$ for all k. The performance of the single-transmitter, single-receiver system using the fixed-threshold acquisition algorithm was previously considered in [3] for communications over an AWGN channel.

2.4.2 Adaptive-Threshold Acquisition Algorithm

The adaptive-threshold algorithm differs from the fixed-threshold algorithm only in that the threshold η_k against which the test statistic X_k is compared differs for different values of k. The adaptive threshold η_k for each sample is given by

$$\eta_k = \frac{\eta^{'} S_k}{\left(\frac{MT_c^2}{\gamma_s \beta}\right)}$$

where $\eta^{'}$ is a predetermined constant. The scaling factor S_k at time $t = kT_c$ given by

$$S_k = \frac{\sum_{q=k-W}^{k-1} X_q}{W}$$

where W is the *window size* of the adaptation algorithm. The performance of the single-transmitter, single-receiver system using the adaptive-threshold acquisition algorithm was

previously considered in [4] for communications over an AWGN channel.

Chapter 3

Acquisition Performance of the Single-Transmitter, Single-Receiver System

The acquisition performance of the single-transmitter, single-receiver system is evaluated in this chapter. It has been evaluated previously for a system operating over an AWGN channel using either fixed-threshold acquisition [3] or adaptive-threshold acquisition [4]. The previous analyses are repeated here for comparison with the new results presented for the dual-transmitter, single-receiver system and the single-transmitter, dual-receiver system in Chapters 4 and 5, respectively. In addition, new results are presented in Section 3.3 for the outage performance of the single-transmitter, single-receiver system in a channel with slow fading. The average performance is evaluated over a random preamble sequence of independent and identically distributed (i.i.d.) quaternary symbols (which we refer to later as a *random preamble sequence*).

3.1 Characterization of the Test Statistics

3.1.1 Matched-Filter Outputs

From equations (2.7) and (2.12), the complex-valued output of the matched filter at $t = kT_c$ is given by

$$\begin{aligned} Z_k &= Z(kT_c) \\ &= (\hat{r} * g)(kT_c) \\ &= Ae^{j\phi}(\hat{s} * g)(kT_c) + (\hat{n} * g)(kT_c) \\ &= S_k + N_k \end{aligned}$$

for $(M - Q) \leq k \leq M$ where

$$S_k = Ae^{j\phi}(\hat{s} * g)(kT_c)$$

and

$$N_k = (\hat{n} * g)(kT_c).$$

Both S_k and N_k are complex-valued random variables; S_k and N_k denote the signal component and the noise component of the sampled matched-filter output, respectively. (The term S_k is a random variable due to the fact that the preamble sequence is random.) The random variables $\{S_{M-Q}, S_{M-Q+1}, ..., S_M\}$ are independent of the random variables $\{N_{M-Q}, N_{M-Q+1}, ..., N_M\}$. From equation (2.8), the signal component is given by

$$\begin{aligned} S_k &= Ae^{j\phi} \int_{-\infty}^{\infty} \sqrt{\alpha(\tau)}\tilde{s}(\tau)(g * \tilde{h})(kT_c - \tau)d\tau \\ &= Ae^{j\phi}\sqrt{P\alpha_1}T_c C_A(M - k) \end{aligned}$$

$$= \frac{AT_c C_A(M-k)e^{j\phi}}{\sqrt{\gamma_s\left(A^2 + \frac{\beta N_0}{PT_c}\right)}} \tag{3.1}$$

where the aperiodic autocorrelation function [9] of the preamble sequence is given by

$$C_A(i) = \begin{cases} \sum_{k=0}^{M-i-1} a_k a_{k+i}^*, & 0 \le i \le M-1 \\ 0, & i \ge M \end{cases}. \tag{3.2}$$

The expectation of the aperiodic autocorrelation function for a random preamble sequence is

$$\mathrm{E}[C_A(M-k)] = \begin{cases} 0, & \mathrm{k} \neq \mathrm{M}, \\ M, & \mathrm{k} = \mathrm{M} \end{cases}. \tag{3.3}$$

From equations (3.3) and (3.1),

$$\mathrm{E}[S_k] = \begin{cases} 0, & k \le M-1 \\ \frac{AMT_c e^{j\phi}}{\sqrt{\gamma_s\left(A^2 + \frac{\beta N_0}{PT_c}\right)}}, & k = M \end{cases}.$$

Also from equation (3.2),

$$\mathrm{E}[C_A(M-j)C_A^*(M-k)] = \begin{cases} k, & j = k \\ 0, & j \neq k \end{cases}. \tag{3.4}$$

The variance of the signal component of the matched-filter output is thus

$$\mathrm{Var}(S_k) = \begin{cases} \frac{A^2 T_c^2 k}{\gamma_s\left(A^2 + \frac{\beta N_0}{PT_c}\right)}, & 0 < k \le M-1 \\ 0, & k = M \text{ and } k \le 0 \end{cases}.$$

Furthermore, $\mathrm{Cov}(S_j, S_k) = 0$ for $j \neq k$ and $\mathrm{Cov}(S_j, S_k^*) = 0$ for all j and k.

The noise component of the matched-filter output is given by

$$N_k = \int_{-(M-k)T_c}^{kT_c} \sqrt{\alpha(\tau)}\tilde{n}(\tau)(g * \tilde{h})(kT_c - \tau)d\tau.$$

The AWGN process $\tilde{n}(t)$ has zero mean; therefore,

$$\mathrm{E}[N_k] = 0, \text{ for all } k.$$

Thus, $\{N_{M-Q}, N_{M-Q+1}, ..., N_M\}$ are zero-mean Gaussian random variables with

$$\mathrm{Var}(N_k) = \begin{cases} \frac{MT_c^2}{\gamma_s \beta}, & k \leq 0 \\ \frac{(M-k)T_c^2}{\gamma_s \beta} + \frac{N_0 k T_c}{\gamma_s P\left(A^2 + \frac{\beta N_0}{PT_c}\right)}, & 0 < k \leq M \end{cases},$$

Furthermore, $\mathrm{Cov}(N_j, N_k) = 0$ for $j \neq k$ and $\mathrm{Cov}(N_j, N_k^*) = 0$ for all j and k. It follows that

$$\begin{aligned} \mathrm{E}[Z_k] &= \mathrm{E}[S_k + N_k] \\ &= \begin{cases} 0, & k \leq M-1 \\ \frac{AMT_c e^{j\phi}}{\sqrt{\gamma_s\left(A^2 + \frac{\beta N_0}{PT_c}\right)}}, & k = M \end{cases}, \end{aligned}$$

$$\begin{aligned} \mathrm{Var}(Z_k) &= \mathrm{Var}(S_k) + \mathrm{Var}(N_k) \\ &= \begin{cases} \frac{MT_c^2}{\gamma_s \beta}, & k \leq 0 \\ \frac{A^2 T_c^2 k}{\gamma_s\left(A^2 + \frac{\beta N_0}{PT_c}\right)} + \frac{(M-k)T_c^2}{\gamma_s \beta} + \frac{N_0 k T_c}{\gamma_s P\left(A^2 + \frac{\beta N_0}{PT_c}\right)}, & 0 < k \leq M-1 \\ \frac{N_0 M T_c}{\gamma_s P\left(A^2 + \frac{\beta N_0}{PT_c}\right)}, & k = M \end{cases}, \end{aligned}$$

Furthermore, $\mathrm{Cov}(Z_j, Z_k) = 0$ for $j \neq k$ and $\mathrm{Cov}(Z_j, Z_k^*) = 0$ for all j and k. That is, the random variables are both uncorrelated and *pseudo-uncorrelated* [10] .

3.1.2 Test Statistics and System Performance

It is shown in [3] and [4] that the performance of the acquisition algorithms is closely approximated if the random variables $\{\mathrm{Re}(Z_{M-Q}), \mathrm{Im}(Z_{M-Q}), \cdots, \mathrm{Re}(Z_M), \mathrm{Im}(Z_M)\}$ are modeled as jointly Gaussian. Since the random variables are uncorrelated and pseudo-uncorrelated, they form a set of mutually independent, complex-valued random variables un-

der the jointly Gaussian approximation; it follows that the test statistics $\{X_{M-Q}, \cdots, X_M\}$ are also independent under the approximation. Furthermore, each test statistic

$$X_k = |\ \mathrm{Re}(Z_k)\ |^2 + |\ \mathrm{Im}(Z_k)\ |^2$$

is a chi-square random variable with two degrees of freedom under the Gaussian approximation. The test statistic X_k is a central chi-square random variable with two degrees of freedom for $M - Q \leq k \leq M - 1$, and X_M is a non-central chi-square random variable with two degrees of freedom [7]. Under the Gaussian approximation, the probability of not acquiring in the fixed-threshold system is thus given by

$$P_{nacq} = 1 - \Pr\left(X_{M-Q} < \eta, \cdots, X_{M-1} < \eta, X_M > \eta\right)$$

$$= 1 - \left[\prod_{k=M-Q}^{M-1} F_{X_k}(\eta)\right](1 - F_{X_M}(\eta)) \tag{3.5}$$

where

$$F_{X_k}(x) = \begin{cases} 1 - e^{-x/2\sigma_k^2}, & k \leq M-1 \\ 1 - Q_1\left(\frac{s_M}{\sigma_M}, \frac{\sqrt{x}}{\sigma_M}\right), & k = M \end{cases},$$

$Q_m(a, b)$ is the generalized Marcum Q-function [7], $s_k^2 = |\ \mathrm{E}[Z_k]\ |^2$, and $\sigma_k^2 = \mathrm{Var}(Z_k)/2$.

3.2 Optimization of the Performance in an AWGN Channel

In a given application, there is some minimum level of acquisition performance which is considered acceptable. It is desirable to design the system to achieve acceptable performance over as wide a range of channel conditions as possible. The fixed-threshold acquisition algorithm has a single design parameter, the threshold η, whereas the adaptive-threshold acquisition algorithm has two design parameters, the threshold parameter η' and the window size W. We consider a specific target probability of not acquiring and optimize the range of AWGN channels over which the target is met or exceeded.

Suppose the fixed-threshold acquisition algorithm is used. For a given choice of η, there is some $SNR_{min}(\eta)$ such that the probability of not acquiring is no greater than the target probability of not acquiring for all AWGN channels with $SNR \geq SNR_{min}(\eta)$. The optimal threshold is given by

$$\eta_{opt} = \arg\min_{\eta} SNR_{min}(\eta)$$

and the corresponding minimum channel quality for acceptable performance is given by

$$SNR^* = \min_{\eta} SNR_{min}(\eta).$$

Similarly for the adaptive-threshold algorithm and a given window size,

$$\eta^{'}_{opt} = \arg\min_{\eta^{'}} SNR_{min}(\eta^{'})$$

and

$$SNR^* = \min_{\eta^{'}} SNR_{min}(\eta^{'}).$$

As shown in [3] and [4], the probability of not acquiring is a non-monotonic function of SNR for a given choice of η or $\eta^{'}$, due to the effect of the AGC subsystem on the received signal. So, the threshold parameter that minimizes the probability of not acquiring at a given signal-to-noise ratio need not necessarily be optimal according to the criterion described above.

The probability of not acquiring is shown in Fig. 3.1 as a function of the instantaneous signal-to-noise ratio for the single-transmitter, single-receiver system using the fixed-threshold acquisition algorithm and using the adaptive-threshold acquisition algorithm with an adaptation window size of $W = 100$. The optimal threshold parameter is used for each algorithm. The chip-pulse waveform and the IF filter result in parameter values $\gamma_s = 1$ and $\beta = 3.0$. The preamble consists of $M = 400$ quaternary chips and the verification interval is 1000 times the chip interval (i.e., $Q = 1000$). (The window size of 100 is nearly optimal

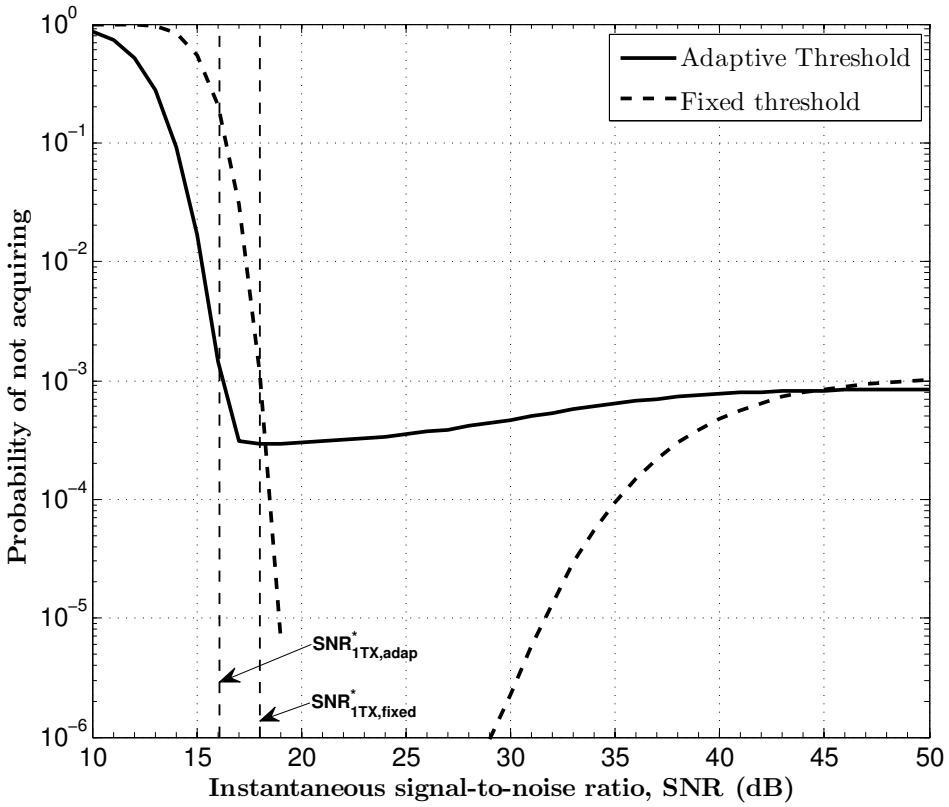

Figure 3.1: Acquisition performance of the single-transmitter, single-receiver system in an AWGN channel.

for the the system parameters considered.) The performance is averaged over all possible choices of the quaternary preamble sequence; it is determined by Monte Carlo simulation using the actual (non-Gaussian) statistics.

The threshold parameters of the two acquisition algorithms are selected to optimize the acquisition performance in the single-transmitter, single-receiver system according to the criterion described above, for a target probability of not acquiring of $P_{nacq} = 1.1 \text{ x } 10^{-3}$. It is observed from Fig. 3.1 that the optimal threshold parameter results in $SNR^*_{1TX1RX,fixed} =$ 18.0 dB for the fixed-threshold algorithm and $SNR^*_{1TX1RX,adap} = 16.1$ dB for the adaptive-threshold algorithm. Thus the adaptive-threshold algorithm results in 1.9 dB better performance than the fixed-threshold algorithm. The performance of the single-transmitter, single-receiver system as approximated by equation (3.5) is indistinguishable from the results of the corresponding Monte Carlo simulation shown in Fig. 3.1.

3.3 Performance in a Time-Varying Channel

The value of SNR^* for a given system specifies the minimum instantaneous signal-to-ratio ratio for which the transmitted packet is acquired with an acceptable probability of not acquiring if the acquisition algorithm uses the optimal value of the corresponding threshold parameter. If the instantaneous signal-to-noise ratio, SNR, falls below SNR^*, the link is said to suffer an *outage*. Thus the probability of outage

$$P_{outage} = \Pr(SNR < SNR^*) \tag{3.6}$$

characterizes the availability of the link.

An expression for the probability of outage of the single-transmitter, single-receiver system operating in a slow Rician-fading channel is derived in Appendix B. The performance is illustrated by considering the system used as an example in Section 3.2 and the optimal threshold for each acquisition algorithm.

The probability of outage in a Rayleigh-fading channel is shown in Fig. 3.2 as a

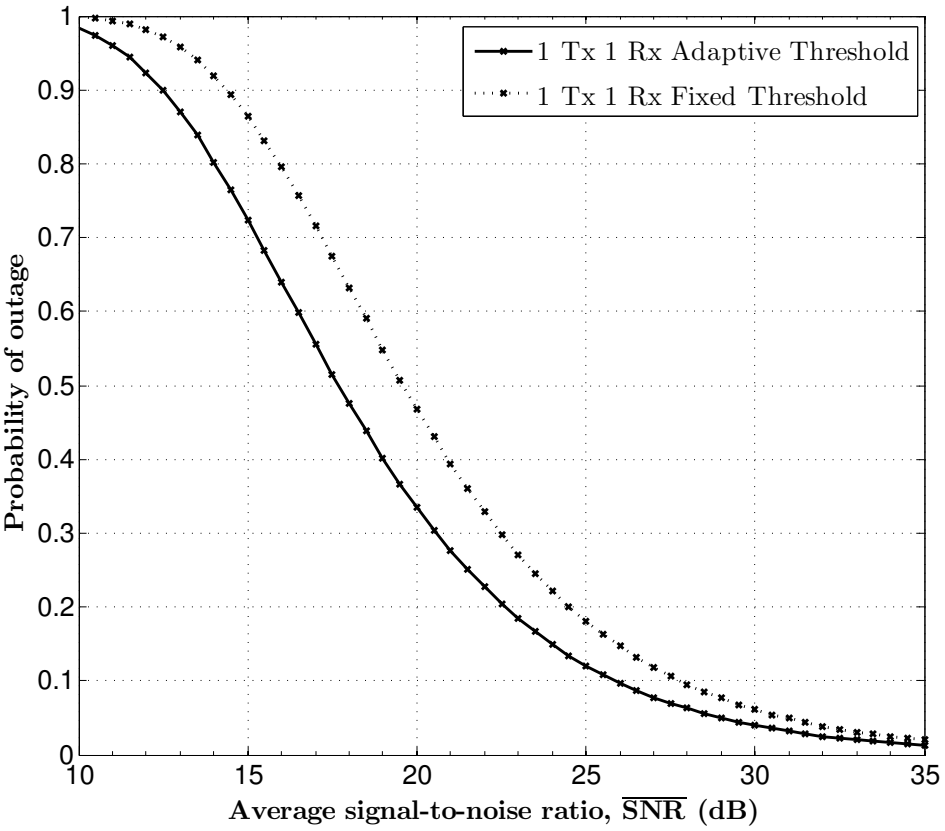

Figure 3.2: Outage probabilities for the single-transmitter, single-receiver system in a Rayleigh-fading channel.

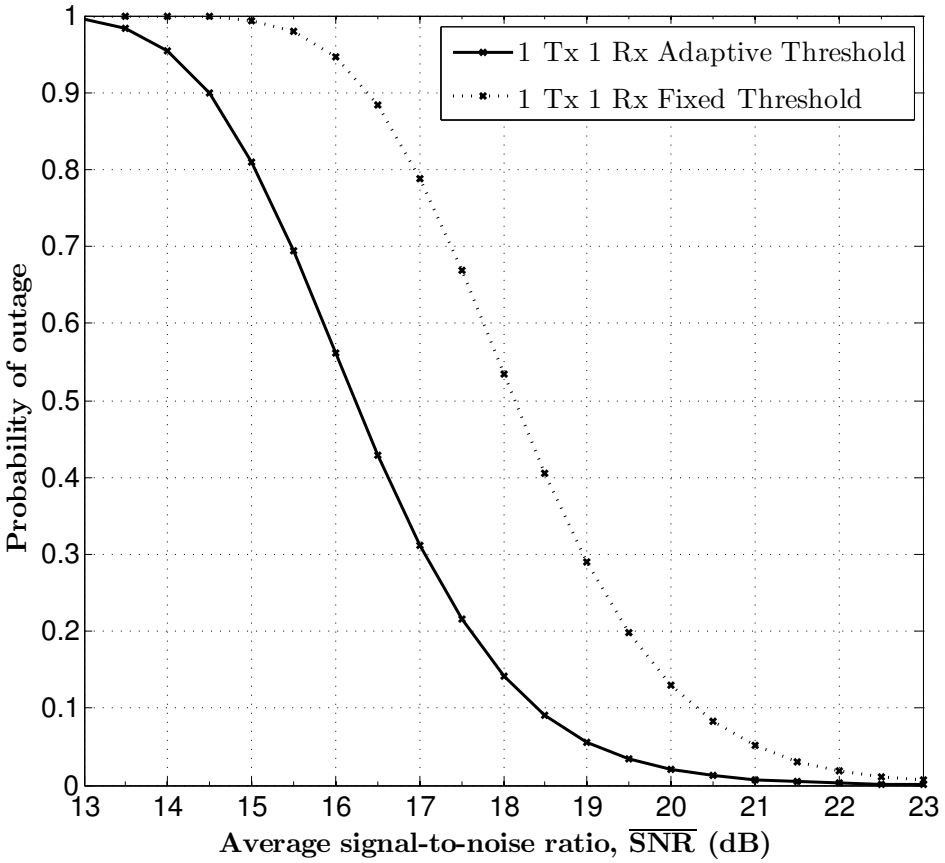

Figure 3.3: Outage probabilities for the single-transmitter, single-receiver system in a Rician-fading channel with a specular-to-diffuse energy ratio of 12 dB.

function of $\overline{SNR}$ for each acquisition algorithm. The adaptive-threshold algorithm results in approximately 1.9 dB better outage performance than the fixed-threshold algorithm in a channel that exhibits Rayleigh fading. For example, for a target probability of outage of 0.1, the fixed-threshold algorithm requires $\overline{SNR} = 27.7$ dB whereas the adaptive-threshold algorithm achieves the same outage probability with $\overline{SNR} = 25.8$ dB.

Suppose instead that the channel exhibits slow Rician fading with a specular-to-diffuse energy ratio of 12 dB. The adaptive-threshold algorithm still provides 1.9 dB better performance than the fixed-threshold algorithm, regardless of the desired probability of outage, as shown in Fig. 3.3.

A further increase in the specular-to-diffuse energy ratio of the channel does not

affect the difference in performance between the adaptive-threshold and fixed-threshold algorithms. In the limit, as the specular-to-diffuse energy ratio approaches infinity (i.e., as the channel approaches a constant-gain AWGN channel), the performance difference between the algorithms remains the same. This can be seen by comparing Figs. 3.2 and 3.3 with Fig. 3.1. In slow, frequency non-selective fading, the adaptive-threshold algorithm performs approximately 1.9 dB better than the fixed-threshold algorithm in the single-transmitter, single-receiver system for any desired outage probability, irrespective of the severity of the fading.

Chapter 4

Acquisition Performance of the Dual-Transmitter, Single-Receiver System

The acquisition performance of the dual-transmitter, single-receiver system is evaluated in this chapter. The test statistics are characterized in Section 4.1 for a random preamble sequence. Optimization of the acquisition performance in an AWGN channel is considered in Section 4.2, and the resulting performance in a channel with slow fading is evaluated in Section 4.3. The performance of the dual-transmitter, single-receiver system is also compared with the performance of the single-transmitter, single-receiver system.

4.1 Characterization of the Test Statistics

4.1.1 Matched Filter Outputs

From equations (2.13) and (2.15), the complex-valued output of the matched filter with impulse response $g_l(t)$, sampled at $t = kT_c$ is given by

$$Z_{l,k} = Z_l(kT_c)$$

$$
\begin{aligned}
&= (\hat{r} * g_l)(kT_c) \\
&= A_l e^{j\phi_l}(\hat{s}_l * g_l)(kT_c) + A_{(l\oplus 1)} e^{j\phi_{(l\oplus 1)}}(\hat{s}_{(l\oplus 1)} * g_l)(kT_c) + (\hat{n} * g_l)(kT_c) \\
&= S_{l,k} + I_{l,k} + N_{l,k}
\end{aligned}
$$

for $(M-Q) \leq k \leq M$, where $\oplus$ indicates modulo-2 addition,

$$
\begin{aligned}
S_{l,k} &= A_l e^{j\phi_l}(\hat{s} * g_l)(kT_c), \\
I_{l,k} &= A_{(l\oplus 1)} e^{j\phi_{(l\oplus 1)}}(\hat{s}_{(l\oplus 1)} * g_l)(kT_c)
\end{aligned}
$$

and

$$
N_{l,k} = (\hat{n} * g_l)(kT_c),
$$

for $l = 0, 1$. The random variables $S_{l,k}$, $I_{l,k}$ and $N_{l,k}$ are all complex-valued for $l = 0, 1$; $S_{l,k}$, $I_{l,k}$ and $N_{l,k}$ denote the signal component, the co-channel interference component and the noise component of the sampled output of the filter with impulse response $g_l(t)$, respectively. The random variables $\{S_{0,M-Q}, S_{1,M-Q}, \cdots, S_{0,M}, S_{1,M}\}$ are independent of the random variables $\{N_{0,M-Q}, N_{1,M-Q}, \cdots, N_{0,M}, N_{1,M}\}$. From equation (2.14), the signal component is given by

$$
\begin{aligned}
S_{l,k} &= A_l e^{j\phi_l} \int_0^{kT_c} \sqrt{\alpha(\tau)}\tilde{s}_l(\tau)(g_l * \tilde{h})(kT_c - \tau)d\tau \\
&= Ae^{j\phi}\sqrt{\frac{P\alpha_1}{2}} T_c C_{A,l}(M-k) \\
&= \frac{A_l T_c C_{A,l}(M-k)e^{j\phi_l}}{\sqrt{2\gamma_s\left(\left(\frac{A_0^2+A_1^2}{2}\right) + \frac{\beta N_0}{PT_c}\right)}}
\end{aligned}
\tag{4.1}
$$

where the aperiodic autocorrelation functions of the orthogonal preamble sequences are given by

$$C_{A,0}(i) = \sum_{k=0}^{M-i-1} a_{0,k}a_{0,k+i}^*$$
$$= \begin{cases} \sum_{k=0}^{(\frac{M-i-2}{2})}[a_{2k}a_{2k+i}^* + a_{2k+1}^*a_{2k+1+i}], & i \text{ even },\ 0 \le i \le M-1 \\ -\sum_{k=0}^{(\frac{M-i-3}{2})}[a_{2k}a_{2k+i} + a_{2k+1}^*a_{2k+1+i}^*] & \\ \qquad -a_{M-i-1}a_{M-1}, & i \text{ odd },\ 0 \le i \le M-1 \\ \qquad 0, & i \ge M \end{cases} \tag{4.2}$$

and

$$C_{A,1}(i) = \sum_{k=0}^{M-i-1} a_{1,k}a_{1,k+i}^*$$
$$= \begin{cases} \sum_{k=0}^{\frac{M-i-2}{2}}[a_{2k+1}a_{2k+1+i}^* + a_{2k}^*a_{2k+i}], & i \text{ even },\ 0 \le i \le M-1 \\ -\sum_{k=0}^{\frac{M-i-3}{2}}[a_{2k+1}a_{2k+i-1} + a_{2k}^*a_{2k+2+i}^*] & \\ \qquad +a_{M-i}a_{M-2}, & i \text{ odd },\ 0 \le i \le M-1 \\ \qquad 0, & i \ge M \end{cases} . \tag{4.3}$$

The expectation of the aperiodic autocorrelation functions for a random preamble sequence $\{a_i\}$ is

$$\mathrm{E}[C_{A,l}(M-k)] = \begin{cases} 0, & \mathrm{k} \neq \mathrm{M}, \\ M, & \mathrm{k} = \mathrm{M} \end{cases} \tag{4.4}$$

for $l = 0, 1$. From equations (4.4) and (4.1),

$$\mathrm{E}[S_{l,k}] = \begin{cases} 0, & k \le M-1 \\ \frac{A_l M T_c e^{j\phi_l}}{\sqrt{2\gamma_s\left(\left(\frac{A_0^2+A_1^2}{2}\right)+\frac{\beta N_0}{PT_c}\right)}}, & k = M \end{cases} .$$

Also from equations (4.2) and (4.3)

$$\mathrm{E}[C_{A,0}(M-j)C^*_{A,0}(M-k)] = \begin{cases} k, & j=k \\ 0, & j\neq k \end{cases}$$

$$\mathrm{E}[C_{A,1}(M-j)C^*_{A,1}(M-k)] = \begin{cases} k, & j=k \\ 0, & j\neq k \end{cases}$$

$$\mathrm{E}[C_{A,0}(M-j)C_{A,1}(M-k)] = \begin{cases} k, & j=k,\ k \text{ even} \\ 0, & \text{otherwise} \end{cases}$$

$$\mathrm{E}[C_{A,0}(M-j)C^*_{A,1}(M-k)] = 0$$

where $0 \leq j \leq M-1$ and $0 \leq k \leq M-1$. The variance of the signal component for $l = 0, 1$ is thus

$$\mathrm{Var}(S_{l,k}) = \begin{cases} \frac{A_l^2 T_c^2 k}{2\gamma_s\left(\left(\frac{A_0^2+A_1^2}{2}\right)+\frac{\beta N_0}{PT_c}\right)}, & 0 < k \leq M-1 \\ 0, & k = M \text{ and } k \leq 0 \end{cases}. \tag{4.5}$$

Furthermore, $\mathrm{Cov}(S_{l_1,j}, S_{l_2,k}) = 0$ if either $l_1 \neq l_2$ or $j \neq k$ where $l_1, l_2 \in \{0, 1\}$, and

$$\mathrm{Cov}(S_{l_1,j}, S^*_{l_2,k}) = \begin{cases} \frac{A_0 A_1 T_c^2 k e^{j(\phi_0+\phi_1)}}{2\gamma_s\left(\left(\frac{A_0^2+A_1^2}{2}\right)+\frac{\beta N_0}{PT_c}\right)}, & l_1 \neq l_2, j = k, 0 < k \leq M-1,\ k \text{ even} \\ 0, & \text{otherwise} \end{cases}.$$

The random variables $\{I_{0,M-Q}, I_{1,M-Q}, \cdots, I_{0,M}, I_{1,M}\}$ are independent of the random variables $\{N_{0,M-Q}, N_{1,M-Q}, \cdots, N_{0,M}, N_{1,M}\}$. The co-channel interference component of the output of the matched-filter with impulse response $g_l(t)$ is given by

$$\begin{aligned} I_{l,k} &= A_{(l\oplus 1)} e^{j\phi_{(l\oplus 1)}} \int_0^{kT_c} \sqrt{\alpha(\tau)}\tilde{s}_{(l\oplus 1)}(\tau)(g_l * \tilde{h})(kT_c - \tau)d\tau \\ &= A_{(l\oplus 1)} e^{j\phi_{(l\oplus 1)}} \sqrt{P\alpha_1/2}T_c C_{C,l\oplus 1,l}(M-k) \end{aligned}$$

$$= \frac{A_{(l\oplus 1)} T_c C_{C,l\oplus 1,l}(M-k) e^{j\phi_{(l\oplus 1)}}}{\sqrt{2\gamma_s \left(\left(\frac{A_0^2 + A_1^2}{2} \right) + \frac{\beta N_0}{P T_c} \right)}} \tag{4.6}$$

where the aperiodic cross-correlation functions [9] of the orthogonal preamble sequences are given by

$$\begin{aligned} C_{C,0,1}(i) &= \sum_{k=0}^{M-i-1} a_{0,k} a_{1,k+i}^* \\ &= \begin{cases} \sum_{k=0}^{\frac{M-i-2}{2}} [a_{2k} a_{2k+1+i}^* - a_{2k+1}^* a_{2k+i}], & i \text{ even },\ 0 \le i \le M-1 \\ -\sum_{k=0}^{\frac{M-i-3}{2}} [a_{2k} a_{2k+i-1} + a_{2k+1}^* a_{2k+2+i}^*] & \\ \qquad + a_{M-i-1} a_{M-2}, & i \text{ odd },\ 0 \le i \le M-1 \\ 0, & i \ge M \end{cases} \end{aligned} \tag{4.7}$$

and

$$\begin{aligned} C_{C,1,0}(i) &= \sum_{k=0}^{M-i-1} a_{1,k} a_{0,k+i}^* \\ &= \begin{cases} \sum_{k=0}^{\frac{M-i-2}{2}} [a_{2k+1} a_{2k+i}^* - a_{2k}^* a_{2k+1+i}], & i \text{ even },\ 0 \le i \le M-1 \\ -\sum_{k=0}^{\frac{M-i-3}{2}} [-a_{2k+1} a_{2k+i} + a_{2k}^* a_{2k+1+i}^*] & \\ \qquad - a_{M-i} a_{M-1}, & i \text{ odd },\ 0 \le i \le M-1 \\ 0, & i \ge M \end{cases} \end{aligned} . \tag{4.8}$$

The expectation of the aperiodic crosscorrelation functions for a uniform distribution on the underlying quaternary sequence $\{a_i\}$ is

$$\mathrm{E}[C_{C,l\oplus 1,l}(M-k)] = 0,\ 0 \le k \le M-1 \tag{4.9}$$

for $l = 0, 1$. From equations (4.9) and (4.6),

$$\mathrm{E}[I_{l,k}] = 0,\ (M-Q) \le k \le M$$

for $l = 0, 1$. Also from equations (4.2),(4.3),(4.7) and (4.8)

$$\mathrm{E}[C_{C,1,0}(M-j)C^*_{C,1,0}(M-k)] = \begin{cases} k, & j = k \\ 0, & j \neq k \end{cases}$$

$$\mathrm{E}[C_{C,0,1}(M-j)C^*_{C,0,1}(M-k)] = \begin{cases} k, & j = k \\ 0, & j \neq k \end{cases}$$

$$\mathrm{E}[C_{C,0,1}(M-j)C_{C,1,0}(M-k)] = \begin{cases} -k, & j = k,\ k \text{ even} \\ 0, & \text{otherwise} \end{cases}$$

$$\mathrm{E}[C_{C,1,0}(M-j)C^*_{C,0,1}(M-k)] = 0$$

$$\mathrm{E}[C_{C,1,0}(M-j)C^*_{A,0}(M-k)] = 0$$

$$\mathrm{E}[C_{C,0,1}(M-j)C^*_{A,0}(M-k)] = 0$$

$$\mathrm{E}[C_{C,1,0}(M-j)C^*_{A,1}(M-k)] = 0$$

$$\mathrm{E}[C_{C,0,1}(M-j)C^*_{A,1}(M-k)] = 0$$

for $0 \leq j \leq M-1$ and $0 \leq k \leq M-1$. Thus, the variance of the interference component for $l = 0, 1$ is

$$\mathrm{Var}(I_{l,k}) = \begin{cases} \frac{A^2_{l\oplus 1} T_c^2 k}{2\gamma_s\left(\left(\frac{A_0^2+A_1^2}{2}\right)+\frac{\beta N_0}{PT_c}\right)}, & 0 < k \leq M-1 \\ 0, & k = M \text{ and } k \leq 0 \end{cases}. \tag{4.10}$$

Furthermore, $\mathrm{Cov}(I_{l_1,j}, I_{l_2,k}) = 0$ if either $l_1 \neq l_2$ or $j \neq k$ where $l_1, l_2 \in \{0, 1\}$, and

$$\mathrm{Cov}(I_{l_1,j}, I^*_{l_2,k}) = \begin{cases} -\frac{A_0 A_1 T_c^2 k e^{j(\phi_0+\phi_1)}}{2\gamma_s\left(\left(\frac{A_0^2+A_1^2}{2}\right)+\frac{\beta N_0}{PT_c}\right)}, & l_1 \neq l_2, j = k, 0 < k \leq M-1,\ k \text{ even} \\ 0, & \text{otherwise} \end{cases}.$$

Also, $\mathrm{Cov}(S_{l_1,j}, I_{l_2,k}) = 0$ for all l_1,l_2,j and k; therefore, the random variables

$$\{S_{0,M-Q}, S_{1,M-Q}, \cdots, S_{0,M}, S_{1,M}\}$$

and the random variables

$$\{I_{0,M-Q}, I_{1,M-Q}, \cdots, I_{0,M}, I_{1,M}\}$$

are mutually uncorrelated. In addition, $\mathrm{Cov}(S_{l_1,j}, I^*_{l_2,k}) = 0$ for all l_1, l_2, j and k. From equations (4.5) and (4.10),

$$\mathrm{Var}(I_{0,k}) = \mathrm{Var}(S_{1,k}) \text{ and } \mathrm{Var}(I_{1,k}) = \mathrm{Var}(S_{0,k});$$

therefore, $\mathrm{Var}(S_{0,k}) + \mathrm{Var}(I_{0,k}) = \mathrm{Var}(S_{1,k}) + \mathrm{Var}(I_{1,k})$, for all k.

The noise component of the output of the filter with impulse response $g_l(t)$ is given by

$$N_{l,k} = \int_{-(M-k)T_c}^{kT_c} \sqrt{\alpha(\tau)}\tilde{n}(\tau)(g_l * \tilde{h})(kT_c - \tau)d\tau$$

for $l = 0, 1$. The AWGN process $\tilde{n}(t)$ has zero mean; therefore

$$\mathrm{E}[N_{l,k}] = 0, \text{ for all } k.$$

Thus, $\{N_{0,M-Q}, N_{1,M-Q}, ..., N_{0,M}, N_{1,M}\}$ are zero-mean Gaussian random variables with

$$\mathrm{Var}(N_{l,k}) = \begin{cases} \frac{MT_c^2}{\gamma_s\beta}, & k \leq 0 \\ \frac{(M-k)T_c^2}{\gamma_s\beta} + \frac{N_0 kT_c}{\gamma_s P\left(\left(\frac{A_0^2+A_1^2}{2}\right)+\frac{\beta N_0}{PT_c}\right)}, & 0 < k \leq M \end{cases}. \tag{4.11}$$

Furthermore, $\mathrm{Cov}(N_{l_1,j}, N_{l_2,k}) = 0$ if either $l_1 \neq l_2$ or $j \neq k$ where $l_1, l_2 \in \{0, 1\}$, and $\mathrm{Cov}(N_{l_1,j}, N^*_{l_2,k}) = 0$ for all l_1, l_2, j and k. Also, from equation (4.11), $\mathrm{Var}(N_{0,k}) = \mathrm{Var}(N_{1,k})$, for all k. It follows that

$$\mathrm{E}[Z_{l,k}] = \mathrm{E}[S_{l,k} + I_{l,k} + N_{l,k}]$$

$$= \begin{cases} 0, & k \leq M-1 \\ \frac{A_l M T_c e^{j\phi_l}}{\sqrt{2\gamma_s\left(\left(\frac{A_0^2+A_1^2}{2}\right)+\frac{\beta N_0}{PT_c}\right)}}, & k = M \end{cases},$$

$$\begin{aligned} \mathrm{Var}(Z_{l,k}) &= \mathrm{Var}(S_{l,k}) + \mathrm{Var}(I_{l,k}) + \mathrm{Var}(N_{l,k}) \\ &= \begin{cases} \frac{MT_c^2}{\gamma_s \beta}, & k \leq 0 \\ \frac{(A_0^2+A_1^2)T_c^2 k}{2\gamma_s\left(\left(\frac{A_0^2+A_1^2}{2}\right)+\frac{\beta N_0}{PT_c}\right)} + \frac{(M-k)T_c^2}{\gamma_s\beta} & \\ \quad + \frac{N_0 k T_c}{\gamma_s P\left(\left(\frac{A_0^2+A_1^2}{2}\right)+\frac{\beta N_0}{PT_c}\right)}, & 0 < k \leq M-1 \\ \frac{N_0 M T_c}{\gamma_s P\left(\left(\frac{A_0^2+A_1^2}{2}\right)+\frac{\beta N_0}{PT_c}\right)}, & k = M \end{cases} \end{aligned}.$$

Furthermore, $\mathrm{Cov}(Z_{l_1,j}, Z_{l_2,k}) = 0$ if either $l_1 \neq l_2$ or $j \neq k$ where $l_1, l_2 \in \{0, 1\}$, and

$$\mathrm{Cov}(Z_{l_1,j}, Z^*_{l_2,k}) = \mathrm{Cov}(S_{l_1,j}, S^*_{l_2,k}) + \mathrm{Cov}(I_{l_1,j}, I^*_{l_2,k}) + \mathrm{Cov}(N_{l_1,j}, N^*_{l_2,k}) = 0$$

for all l_1, l_2, j and k.

4.1.2 Test Statistics and System Performance

As for the single-transmitter, single-receiver system, the performance of the acquisition algorithms is closely approximated if the random variables

$$\{\mathrm{Re}(Z_{0,M-Q}), \mathrm{Im}(Z_{0,M-Q}), \cdots, \mathrm{Re}(Z_{1,M}), \mathrm{Im}(Z_{1,M})\}$$

are modeled as jointly Gaussian. Since the random variables are mutually uncorrelated and mutually pseudo-uncorrelated, they form a set of independent, complex-valued random variables under the Gaussian approximation; it follows that the test statistics $\{X_{M-Q}, ..., X_M\}$ are also independent under the approximation. Furthermore, each test statistic

$$X_k = |Z_{0,k}|^2 + |Z_{1,k}|^2,$$

is a chi-square random variable with four degrees of freedom. The test statistic X_k is a central chi-square random variable with four degrees of freedom for $M-Q \leq k \leq M-1$, and X_M is a non-central chi-square random variable with four degrees of freedom. Under the Gaussian approximation, the probability of not acquiring in the fixed-threshold system is thus given by

$$P_{nacq} = 1 - \Pr\left(X_{M-Q} < \eta, \cdots, X_{M-1} < \eta, X_M > \eta\right)$$

$$= 1 - \left[\prod_{k=M-Q}^{M-1} F_{X_k}(\eta)\right]\left(1 - F_{X_M}(\eta)\right) \tag{4.12}$$

where

$$F_{X_k}(x) = \begin{cases} 1 - e^{-x/2\sigma_k^2} - \frac{x}{2\sigma_k^2} e^{-x/2\sigma_k^2}, & k \leq M-1 \\ 1 - Q_2\left(\frac{s_M}{\sigma_M}, \frac{\sqrt{x}}{\sigma_M}\right), & k = M \end{cases},$$

$Q_m(a,b)$ is the generalized Marcum Q-function, $s_k^2 = |\ \mathrm{E}[Z_{0,k}]\ |^2 + |\ \mathrm{E}[Z_{1,k}]\ |^2$, and $\sigma_k^2 = \mathrm{Var}(Z_{0,k})/2 = \mathrm{Var}(Z_{1,k})/2$.

4.2 Optimization of the Performance in an AWGN Channel

As discussed in Chapter 3 for the single-transmitter, single-receiver system, we would like to choose the parameters η and $\eta^{'}$ for the dual-transmitter system using fixed and adaptive thresholds, respectively, to yield acceptable acquisition performance over as wide a range of channel conditions as possible. For a given choice of the threshold and the window size, the performance of the dual-transmitter system depends only on the instantaneous signal-to-noise ratio (SNR) at the receiver and not on the individual channel gains. Therefore, the method for choosing an optimal threshold for the dual transmitter system is the same as for the single-transmitter, single-receiver system. The optimal thresholds η_{opt} for the fixed-threshold acquisition algorithm and $\eta_{opt}^{'}$ for the adaptive-threshold acquisition algorithm are chosen using the criterion described in Section 3.2. As seen in Fig. 4.1, the probability

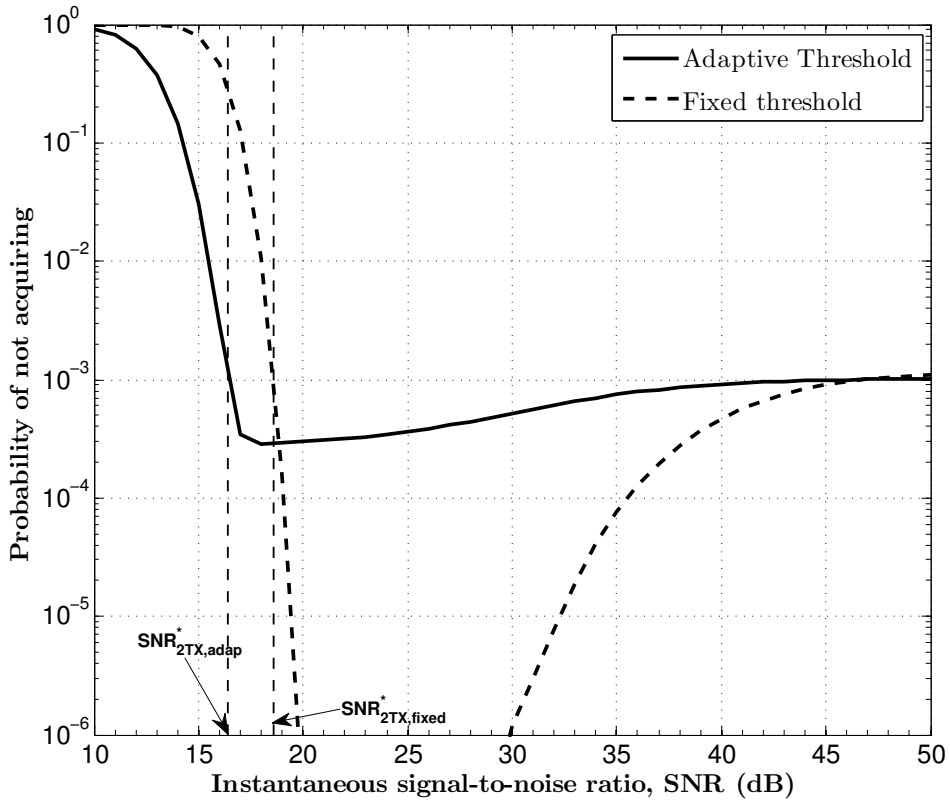

Figure 4.1: Acquisition performance of the dual-transmitter, single-receiver system in an AWGN channel.

of not acquiring for the dual-transmitter system is also a non-monotonic function of SNR, for a given choice of η or $\eta^{'}$. Thus, the threshold parameter that minimizes the probability of not acquiring at a given signal-to-noise ratio need not necessarily be optimal.

The probability of not acquiring as a function of the instantaneous signal-to-noise ratio for the dual-transmitter, single-receiver system using the fixed-threshold acquisition algorithm and using the adaptive-threshold acquisition algorithm with an adaptation window size of $W = 100$ is shown in Fig. 4.1. The optimal threshold parameter is used for each system. The chip-pulse waveform and IF filter result in parameter values $\gamma_s = 1$ and $\beta = 3.0$. The preamble consists of $M = 400$ quaternary chips and the verification interval is 1000 times the chip interval (i.e., $Q = 1000$). (The window size $W = 100$ is nearly optimal for the the system parameters considered.) The performance is averaged over all possible choices of quaternary preamble sequences; it is determined by Monte Carlo simulation using the actual (non-Gaussian) statistics.

The threshold parameters of the two acquisition algorithms are selected to optimize the acquisition performance according to the criterion described in Section 3.2, for a target probability of not acquiring of 1.1 x 10^{-3}. As shown in Fig. 4.1, the optimal threshold parameter results in $SNR^{*}_{2TX1RX,fixed} = 18.6$ dB for the fixed-threshold algorithm and $SNR^{*}_{2TX1RX,adap} = 16.4$ dB for the adaptive-threshold algorithm. Thus the adaptive-threshold algorithm results in 2.2 dB better performance than the fixed-threshold algorithm. For each algorithm, the performance of the dual-transmitter, single-receiver system is a few tenths of one decibel poorer than the performance of the single-transmitter, single-receiver system. This is a result of the non-coherent combining loss [11] suffered in forming the test statistics for the dual-transmitter, single-receiver system. The performance of the dual-transmitter single-receiver system as described by equation (4.12) is indistinguishable from the results of the corresponding Monte Carlo simulation shown in Fig. 4.1.

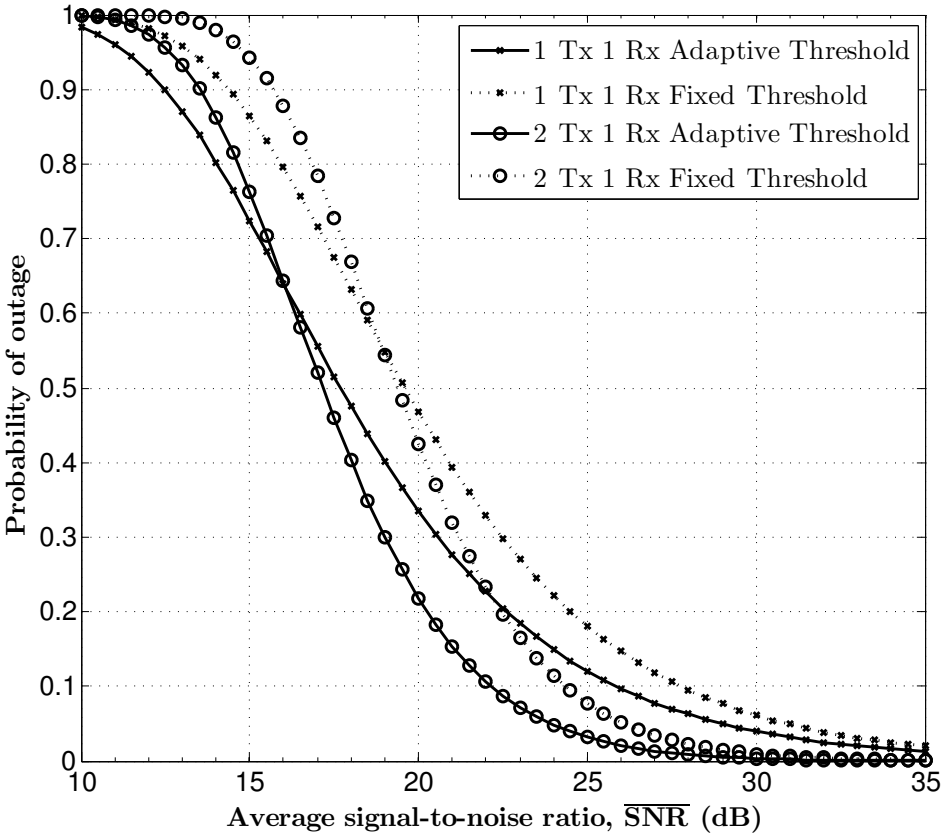

Figure 4.2: Outage probabilities for the dual-transmitter, single-receiver system in a Rayleigh-fading channel.

4.3 Performance in a Time-Varying Channel

The probability of outage in the dual-transmitter, single-receiver system is defined in the same way as for the single-transmitter, single-receiver system in Section 3.3. The expression for the probability of outage of the dual-transmitter, single-receiver system operating in a slow Rician-fading channel is derived in Appendix B. The performance is illustrated by considering the system used as an example in Section 4.2 and the optimal threshold for each acquisition algorithm.

The probability of outage for the single-transmitter, single-receiver system and the dual-transmitter, single-receiver system in a Rayleigh-fading channel is shown in Fig. 4.2 as a function of $\overline{SNR}$ for each acquisition algorithm. In the dual-transmitter, single-receiver

system, the adaptive-threshold algorithm results in approximately 2.2 dB better outage performance than the fixed-threshold algorithm. For example, for an target probability of outage of 0.1, the fixed-threshold algorithm requires $\overline{SNR} = 24.3$ dB whereas the adaptive-threshold algorithm achieves the same outage probability with $\overline{SNR} = 22.1$ dB. The corresponding values for the single-transmitter system are $\overline{SNR} = 27.7$ dB with a fixed threshold and $\overline{SNR} = 25.8$ dB with an adaptive threshold.

For a target outage probability of 0.1, the dual-transmitter system is thus approximately 3.4 dB better than the single-transmitter system when the optimal fixed threshold is used and approximately 3.7 dB better than the single-transmitter system when the optimal adaptive threshold parameter is used. The dual diversity achieved with the two-transmitter system provides an increased robustness against fading that more than offsets the receiver's non-coherent combining loss during acquisition, thus resulting in better performance than the single-transmitter system at outage probabilities of practical interest for a Rayleigh-fading channel. The performance gap between the dual-transmitter and the single-transmitter system expressed in decibels increases as a more stringent condition for the outage probability is imposed.

Suppose instead that the channel exhibits slow Rician fading with a specular-to-diffuse energy ratio of 12 dB. Once again, the adaptive-threshold algorithm provides 2.2 dB better performance than the fixed-threshold algorithm, regardless of the desired probability of outage. This is seen in Fig. 4.3. In contrast, the diversity benefits of the two-transmitter system become less significant as the severity of channel fading decreases, and its performance advantage over the single-transmitter system diminishes accordingly. This is again shown in Fig. 4.3. The average signal-to-noise ratio required to achieve an outage probability of 0.1 for the two-transmitter system is only 0.6 dB lower than for the single-transmitter system if the adaptive-threshold algorithm is used and only 0.2 dB lower if a fixed threshold is used.

A further increase in the specular-to-diffuse energy ratio of the channel does not affect the difference in performance between the adaptive-threshold and fixed-threshold

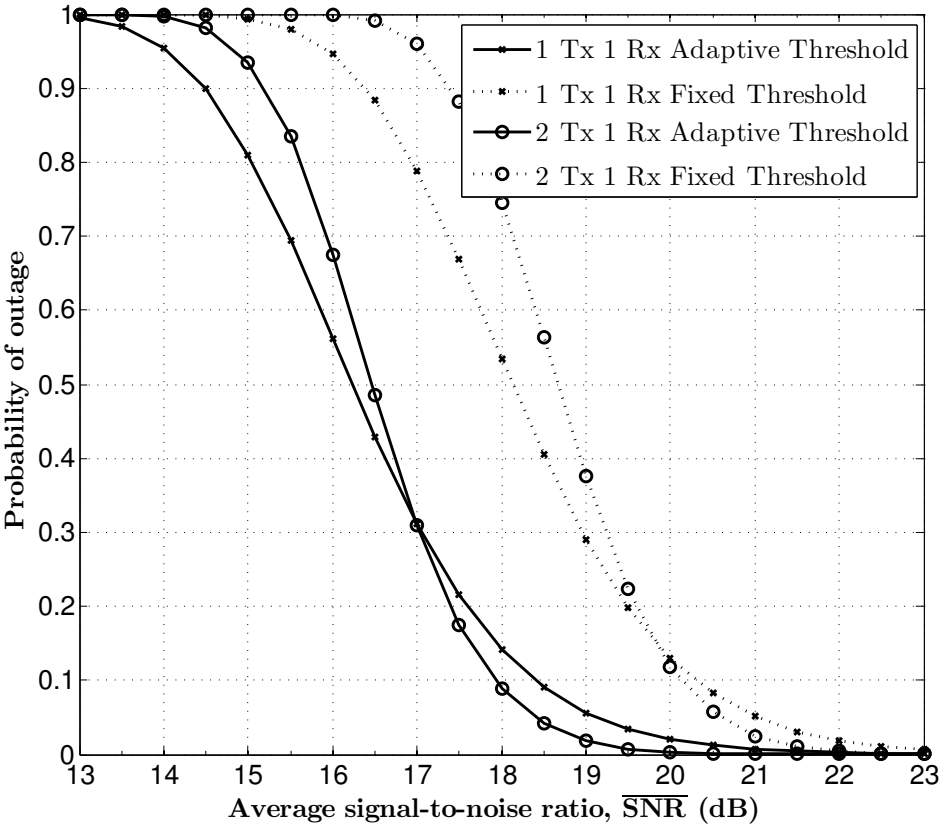

Figure 4.3: Outage probabilities for the dual-transmitter, single-receiver system in a Rician-fading channel with a specular-to-diffuse energy ratio of 12 dB.

algorithms. In the limit, as the specular-to-diffuse energy ratio approaches infinity (i.e., as the channel approaches a constant-gain AWGN channel), the performance approaches that illustrated in Fig. 4.1, in which the single-transmitter system performs better than the dual-transmitter system by 0.6 dB if fixed threshold is used and by 0.3 dB if adaptive threshold is used. Therefore, the effect of the non-coherent combining loss outweighs the benefits of transmission diversity if the specular-to-diffuse energy ratio is very large.

Chapter 5

Acquisition Performance of the Single-Transmitter, Dual-Receiver System

The acquisition performance of the single-transmitter, dual-receiver system is evaluated in this chapter. The test statistics are characterized in Section 5.1 for a random preamble sequence. Optimization of the acquisition performance in an AWGN channel is considered in Section 5.2, and the resulting performance in a channel with slow fading is evaluated in Section 5.3. The performance of the single-transmitter, dual-receiver system is compared with the performance of the single-transmitter, single-receiver system and the dual-transmitter, single-receiver system. The effect of the noise degradation factor on the performance of the single-transmitter, dual-receiver system is also examined.

5.1 Characterization of the Test Statistics

5.1.1 Matched Filter Outputs

From equations (2.16) and (2.12), the complex-valued output of the matched filter in receiver chain l at $t = kT_c$ is given by

$$\begin{aligned} Z_{l,k} &= Z_l(kT_c) \\ &= (\hat{r}_l * g)(kT_c) \\ &= A_l e^{j\phi_l}(\hat{s}_l * g)(kT_c) + (\hat{n}_l * g)(kT_c) \\ &= S_{l,k} + N_{l,k} \end{aligned}$$

for $(M - Q) \leq k \leq M$ where

$$S_{l,k} = A_l e^{j\phi_l}(\hat{s}_l * g)(kT_c)$$

and

$$N_{l,k} = (\hat{n}_l * g)(kT_c),$$

for $l = 0, 1$. The random variables $S_{l,k}$ and $N_{l,k}$ are complex-valued for $l = 0, 1$; $S_{l,k}$ and $N_{l,k}$ denote the signal component and the noise component of the sampled matched-filter output in receiver chain l, respectively. The random variables $\{S_{l,M-Q}, \cdots, S_{l,M}\}$ are independent of the random variables $\{N_{l,M-Q}, \cdots, N_{l,M}\}$ for $l = 0, 1$. From equation (2.17), the signal component in receiver chain l is given by

$$\begin{aligned} S_{l,k} &= A_l e^{j\phi_l} \int_{-\infty}^{\infty} \sqrt{\alpha_l(\tau)}\tilde{s}(\tau)(g * \tilde{h}_l)(kT_c - \tau)d\tau \\ &= A_l e^{j\phi_l} \sqrt{P\alpha_{l,1}} T_c C_A (M - k) \end{aligned}$$

$$= \frac{\sqrt{G_l} A_l T_c C_A(M-k) e^{j\phi_l}}{\sqrt{\gamma_s \left(A_l^2 + \frac{\beta_l N_l}{PT_c} \right)}} \tag{5.1}$$

where the aperiodic autocorrelation function $C_A(i)$ of the preamble sequence is defined in equation (3.2). From equations (3.3) and (5.1),

$$\mathrm{E}[S_{l,k}] = \begin{cases} 0, & k \leq M-1 \\ \frac{\sqrt{G_l} A_l M T_c e^{j\phi_l}}{\sqrt{\gamma_s \left(A_l^2 + \frac{\beta_l N_l}{PT_c} \right)}}, & k = M \end{cases}$$

for $l \in \{0, 1\}$. From equation (3.4), the variance of the signal component of the matched-filter output is

$$\mathrm{Var}(S_{l,k}) = \begin{cases} \frac{G_l A_l^2 T_c^2 k}{\gamma_s \left(A_l^2 + \frac{\beta_l N_l}{PT_c} \right)}, & 0 < k \leq M-1 \\ 0, & k = M \text{ and } k \leq 0 \end{cases}$$

for $l \in \{0, 1\}$ and

$$\mathrm{Cov}(S_{l_1,j}, S_{l_2,k}) = \begin{cases} \frac{\sqrt{G_0 G_1} A_0 A_1 k T_c^2 e^{j(\phi_0 - \phi_1)}}{\gamma_s \sqrt{\left(A_0^2 + \frac{\beta_0 N_0}{PT_c} \right) \left(A_1^2 + \frac{\beta_1 N_1}{PT_c} \right)}}, & l_1 \neq l_2 \text{ and } j = k \\ 0, & j \neq k \end{cases} . \tag{5.2}$$

where $l_1, l_2 \in \{0, 1\}$. Furthermore, $\mathrm{Cov}(S_{l_1,j}, S^*_{l_2,k}) = 0$ for all l_1, l_2, j and k.

The noise component of the matched-filter output in receiver chain l is given by

$$N_{l,k} = \int_{-(M-k)T_c}^{kT_c} \sqrt{\alpha_l(\tau)} \tilde{n}_l(\tau) (g * \tilde{h}_l)(kT_c - \tau) d\tau$$

for $l \in \{0, 1\}$. The AWGN processes $\tilde{n}_0(t)$ and $\tilde{n}_1(t)$ are independent and have zero-mean; therefore

$$\mathrm{E}[N_{l,k}] = 0 \text{ for all } k \text{ and } l \in \{0, 1\}$$

Thus, $\{N_{0,M-Q}, N_{1,M-Q}, \cdots, N_{0,M}, N_{1,M}\}$ are zero-mean Gaussian random variables with

$$\mathrm{Var}(N_{l,k}) = \begin{cases} \frac{G_l M T_c^2}{\gamma_s \beta_l}, & k \leq 0 \\ \frac{G_l (M-k) T_c^2}{\gamma_s \beta_l} + \frac{G_l N_l k T_c}{\gamma_s P \left(A_l^2 + \frac{\beta_l N_l}{P T_c} \right)}, & 0 < k \leq M \end{cases}$$

for $l \in \{0, 1\}$, and $\mathrm{Cov}(N_{l_1,j}, N_{l_2,k}) = 0$ if either $l_1 \neq l_2$ or $j \neq k$ where $l_1, l_2 \in \{0, 1\}$. Furthermore, $\mathrm{Cov}(N_{l_1,j}, N_{l_2,k}) = 0$ for all l_1, l_2, j and k. It follows that

$$\begin{aligned} \mathrm{E}[Z_{l,k}] &= \mathrm{E}[S_{l,k} + N_{l,k}] \\ &= \begin{cases} 0, & k \leq M-1 \\ \frac{\sqrt{G_l} A_l M T_c e^{j\phi_l}}{\sqrt{\gamma_s \left(A_l^2 + \frac{\beta_l N_l}{P T_c} \right)}}, & k = M \end{cases}, \end{aligned}$$

$$\begin{aligned} \mathrm{Var}(Z_{l,k}) &= \mathrm{Var}(S_{l,k}) + \mathrm{Var}(N_{l,k}) \\ &= \begin{cases} \frac{G_l M T_c^2}{\gamma_s \beta_l}, & k \leq 0 \\ \frac{G_l A_l^2 T_c^2 k}{\gamma_s \left(A_l^2 + \frac{\beta_l N_l}{P T_c} \right)} + \frac{G_l (M-k) T_c^2}{\gamma_s \beta_l} + \frac{G_l N_l k T_c}{\gamma_s P \left(A_l^2 + \frac{\beta_l N_l}{P T_c} \right)}, & 0 < k \leq M-1 \\ \frac{N_l M T_c}{\gamma_s P \left(A_l^2 + \frac{\beta_l N_l}{P T_c} \right)}, & k = M \end{cases} \end{aligned} \tag{5.3}$$

for $l \in \{0, 1\}$, and

$$\mathrm{Cov}(Z_{l_1,j}, Z_{l_2,k}) = \mathrm{Cov}(S_{l_1,j}, S_{l_2,k}), \tag{5.4}$$

for $l_1, l_2 \in \{0, 1\}$. Furthermore, $\mathrm{Cov}(Z_{l_1,j}, Z^*_{l_2,k}) = 0$ for all l_1, l_2, j and k.

5.1.2 Test Statistics and System Performance

As for the single-receiver systems, the performance of the acquisition algorithms is closely approximated if the random variables

$$\{\mathrm{Re}(Z_{0,M-Q}), \mathrm{Im}(Z_{0,M-Q}), \cdots, \mathrm{Re}(Z_{1,M}), \mathrm{Im}(Z_{1,M})\}$$

are modeled as jointly Gaussian. Since the random variables $Z_{l_1,j}$ and $Z_{l_2,k}$ are uncorrelated for $j \neq k$, they form a set of independent random variables under the Gaussian approximation, where l_1 and l_2 can be 0 or 1. It follows that the test statistics $\{X_{M-Q}, \cdots, X_M\}$ are also independent under the approximation. From equation (5.4) it is clear that for $0 < k \leq M-1$ the matched-filter outputs in the two receiver chains, $Z_{0,k}$ and $Z_{1,k}$, are correlated. However, for $k \leq 0$ and $k = M$, the random variables $Z_{0,k}$ and $Z_{1,k}$ are uncorrelated. Also $Z_{0,k}$ and $Z_{1,k}$ may have unequal variances in general due to the difference in the receiver chain and channel characteristics. Thus, the test statistic given by

$$X_k = |Z_{0,k}|^2 + |Z_{1,k}|^2$$

is a sum of two chi-square random variables with two degrees of freedom. Under the Gaussian approximation, the probability of not acquiring in the fixed-threshold system is thus given by

$$P_{nacq} = 1 - \Pr\left(X_{M-Q} < \eta, \cdots, X_{M-1} < \eta, X_M > \eta\right)$$

$$= 1 - \left[\prod_{k=M-Q}^{M-1} F_{X_k}(\eta)\right] (1 - F_{X_M}(\eta)) \tag{5.5}$$

where $F_{X_k}(x)$ is the cumulative distribution function of the test statistics. The distribution function $F_{X_k}(x)$ is evaluated below for each statistic X_k with $s_{l,k}^2 = |\ \mathrm{E}[Z_{l,k}]\ |^2$ and $\sigma_{l,k}^2 = \mathrm{Var}(Z_{l,k})/2$, for $l \in \{0, 1\}$.

The test statistic X_k is the sum of two uncorrelated central chi-square random variables with two degrees of freedom and unequal variances, for $k \leq 0$. (In the special case where the RF front-end electronics of the receivers have identical components and the two channels have the same gain (i.e., $A_0 = A_1$), the two chi-square random variables have equal variances so that X_k is a central chi-square random variable with four degrees of freedom.) The distribution function for the sum of two uncorrelated central chi-square

random variables with two degrees of freedom is given by

$$F_{X_k}(x) = \begin{cases} \frac{\sigma_{0,k}^2 F_{X_{0,k}}(x) - \sigma_{1,k}^2 F_{X_{1,k}}(x)}{\sigma_{0,k}^2 - \sigma_{1,k}^2}, & \sigma_{0,k} \neq \sigma_{1,k} \\ 1 - e^{-x/2\sigma_k^2} - \frac{x}{2\sigma_k^2} e^{-x/2\sigma_k^2}, & \sigma_{0,k} = \sigma_{1,k} = \sigma_k \end{cases}$$

where $F_{X_{l,k}}(x) = 1 - e^{-x/2\sigma_{l,k}^2}$ for $l = 0, 1$ is the distribution of a central chi-square random variable with two degrees of freedom.

For $k = M$, X_k is the sum of two uncorrelated non-central chi-square random variables with two degrees of freedom. The distribution function for X_M can be obtained as an integral and evaluated numerically. (In the special case where the RF front-end electronics of the receivers have identical components and the two channels have the same gain, the two non-central chi-square random variables have equal variances and X_k is a non-central chi-square random variable with four degrees of freedom.) For $k = M$, the distribution of X_k is given by

$$F_{X_M}(x) = \begin{cases} \int_0^x F_{X_{0,M}}(x-y) f_{X_{1,M}}(y) dy, & \sigma_{0,M} \neq \sigma_{1,M} \\ 1 - Q_2\left(\frac{s_M}{\sigma_{0,M}}, \frac{\sqrt{\eta}}{\sigma_{0,M}}\right), & \sigma_{0,M} = \sigma_{1,M} \end{cases}$$

where

$$F_{X_{0,M}}(x) = 1 - Q_1\left(\frac{s_{0,M}}{\sigma_{0,M}}, \frac{\sqrt{x}}{\sigma_{0,M}}\right),$$

$$f_{X_{1,M}}(x) = \frac{1}{2\sigma_{1,M}^2} e^{-\frac{s_{1,M}^2 + x}{2\sigma_{1,M}^2}} I_0\left(\frac{\sqrt{x} s_{1,M}}{\sigma_{1,M}^2}\right),$$

$Q_m(a, b)$ is the generalized Marcum Q-function and $I_n(z)$ is the n^{th} order modified Bessel function of the first kind [7].

For $0 < k \leq M-1$, the test statistic X_k is a sum of two correlated central chi-square random variables with two degrees of freedom. By an appropriate transformation of the variables as described in Appendix A, X_k can be expressed as the sum of two independent

chi-square random variables with two degrees of freedom. Specifically

$$X_k = X_{0,k} + X_{1,k} = |Y_{0,k}|^2 + |Y_{1,k}|^2$$

where $Y_{0,k}$ and $Y_{1,k}$ are independent, zero-mean, complex-valued Gaussian random variables with respective variances

$$\lambda_1 = (\mathrm{Var}(Z_{0,k}) + \mathrm{Var}(Z_{1,k}) - \Delta)/2$$

and

$$\lambda_2 = (\mathrm{Var}(Z_{0,k}) + \mathrm{Var}(Z_{1,k}) + \Delta)/2$$

where

$$\Delta = \sqrt{(\mathrm{Var}(Z_{0,k}) - \mathrm{Var}(Z_{1,k}))^2 + 4 \mid \mathrm{Cov}(Z_{0,k}, Z_{1,k}) \mid^2}.$$

The random variables $X_{0,k}$ and $X_{1,k}$ are thus independent, central, chi-square random variables with two degrees of freedom. Therefore,

$$F_{X_k}(x) = \frac{\lambda_2 F_{X_{0,k}}(x) - \lambda_1 F_{X_{1,k}}(x)}{\lambda_2 - \lambda_1} \tag{5.6}$$

where $F_{X_{0,k}}(x) = 1 - e^{-x/\lambda_2}$ and $F_{X_{1,k}}(x) = 1 - e^{-x/\lambda_1}$. The expression in equation (5.6) holds good irrespective of whether or not $\sigma_{1,k}$ and $\sigma_{0,k}$ are equal.

5.2 Optimization of the Performance in an AWGN Channel

As discussed in Chapters 3 and 4 for the single-receiver systems, it is desirable to choose the parameters η and $\eta^{'}$ for the dual-receiver system using fixed and adaptive thresholds, respectively, to achieve acceptable performance over as wide a range of channel conditions as possible. For a given choice of threshold and the window size, the performance of the dual-receiver system depends not only on the instantaneous signal-to-noise ratio (SNR) at the receiver, however, but also on the ratio of the channel gains.

Two approaches can be taken to optimizing the acquisition threshold parameter η or $\eta^{'}$. They are illustrated by considering the selection of the threshold for the fixed-threshold algorithm. Suppose the random variable $B_0 = A_0^2/A_1^2$ denotes the squared ratio of the channel gains. For a given threshold η, there is some signal-to-noise ratio $SNR_{min}(B_0, \eta)$ above which an acceptable probability of not acquiring is achieved.

The first approach to threshold optimization is intended to exploit the channel efficiently under the broadest possible range of conditions. It is an idealized approach that assumes *a priori* knowledge of the channel-gain ratio (though not the signal-to-noise ratio). The optimal threshold for a given value of B_0 is

$$\tilde{\eta}_{opt}(B_0) = \arg\min_{\eta} SNR_{min}(B_0, \eta).$$

Acceptable performance is achieved in channels with a channel-gain ratio B_0 if the signal-to-noise ratio is at least

$$\widetilde{SNR}^{*}(B_0) = SNR_{min}(B_0, \tilde{\eta}_{opt}(B_0)).$$

The second approach is practical in that it does not require *a priori* knowledge of either the channel-gain ratio or the signal-to-noise ratio. It ensures that acceptable performance is achieved over the widest possible range of signal-to-noise ratios irrespective of the channel-gain ratio. The optimal threshold is given by

$$\eta_{opt} = \arg\min_{\eta} \max_{B_0} SNR_{min}(B_0, \eta). \tag{5.7}$$

With this threshold, acceptable performance is achieved if the signal-to-noise ratio exceeds

$$SNR^{*} = \max_{B_0} SNR_{min}(B_0, \eta_{opt}) \tag{5.8}$$

For the single-transmitter, dual-receiver system containing receiver chains using

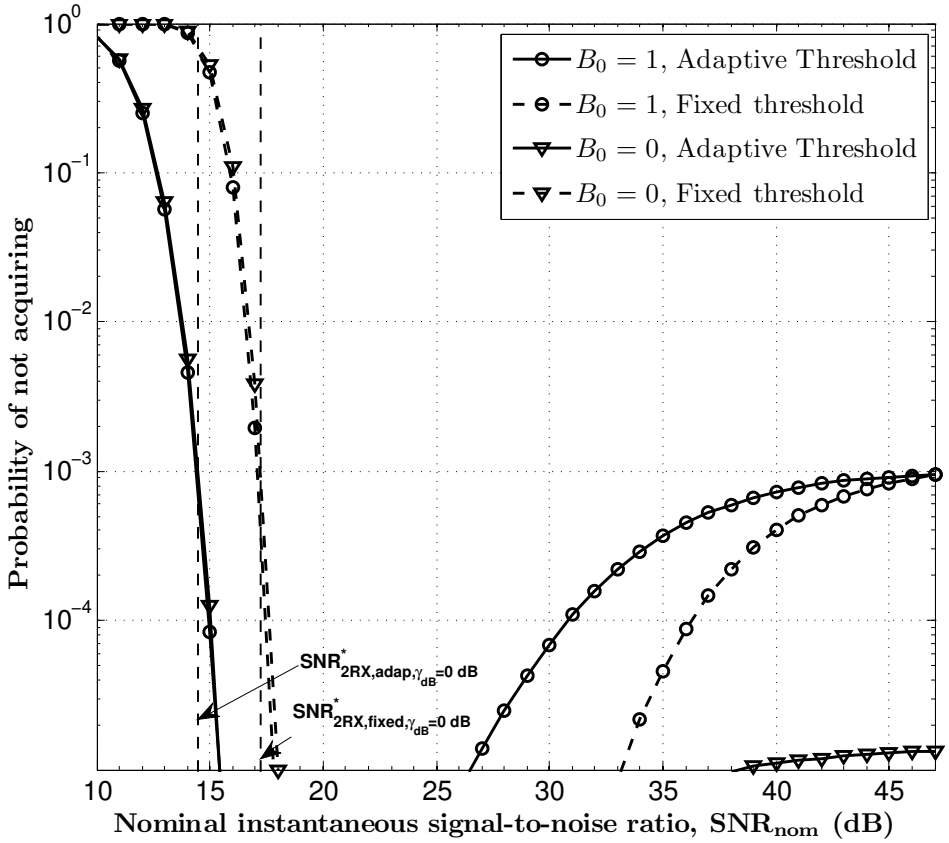

Figure 5.1: Acquisition performance of the single-transmitter, dual-receiver system in an AWGN channel with $\gamma_{dB} = 0$ dB.

RF and IF components with the same characteristics, SNR^* is only slightly greater than $\min_{B_0} \widetilde{SNR}^*(B_0)$. (They differ by at most 0.15 dB in the examples we have considered and the resulting difference in performance for most channels of interest is even less.) Thus we use the optimality criterion of equation (5.7) in all that follows.

As shown in Fig. 5.1, the probability of not acquiring for the dual-receiver system also is a non-monotonic function of SNR, for a given value of B_0 and a given choice of η or η'. So the threshold parameter that minimizes the probability of not acquiring at a given signal-to-noise ratio and B_0 need not necessarily be optimal.

The probability of not acquiring is shown in Fig. 5.1 as a function of the instantaneous signal-to-noise ratio for the single-transmitter, dual-receiver system and both acqui-

sition algorithms. Performance is shown for constant-gain channels with two gain ratios: $B_0 = 1$ (equal-gain channels) and $B_0 = 0$ (gain of zero in channel zero). The window size of the adaptive-threshold algorithm is 100, which is nearly optimal for the system parameters considered. The chip-pulse waveform and IF filter result in parameter values $\gamma_s = 1$ and $\beta_0 = \beta_1 = 3.0$. The average output powers of the AGC subsystems in the two receiver chains are assumed to be equal (i.e. $G_0 = G_1$). The preamble consists of $M = 400$ quaternary chips and the verification interval is chosen to be 1000 times the chip interval (which corresponds to a choice of $Q = 1000$). The noise power spectral densities in the RF front-end of of the two receiver chains are considered to be equal (i.e., the noise factor degradation $\gamma_{dB} = 0$ dB). The performance is averaged over all possible choices of quaternary preamble sequences; it is determined by Monte Carlo simulation using the actual (non-Gaussian) statistics.

The threshold parameters of the two acquisition algorithms are selected to optimize the acquisition performance according to the criterion described above, for a target probability of not acquiring of 1.1 x 10^{-3}. It is observed from Fig. 5.1 that the choice of optimal threshold results in $SNR^*_{1TX2RX,fixed} = 17.3$ dB for the fixed-threshold algorithm and $SNR^*_{1TX2RX,adap} = 14.5$ dB for the adaptive-threshold algorithm. Thus the adaptive-threshold algorithm results in 2.8 dB better performance than the fixed-threshold algorithm. Note that the performance of the dual-transmitter single-receiver system as described by equation (5.5) is indistinguishable from the results of the Monte Carlo simulation shown in Fig. 5.1.

Now consider all three systems operating over the same equal-gain channels. The performance of the single-transmitter, dual-receiver system is better than that of the dual-transmitter, single-receiver system by 1.3 dB if the fixed-threshold algorithm is used and by 1.9 dB is the adaptive-threshold algorithm is used. The corresponding improvement in performance using the single-transmitter, dual-receiver system over the single-transmitter, single-receiver system is 0.7 dB and 1.6 dB using fixed and adaptive thresholds, respectively. One would expect the dual-receiving antenna diversity system to ideally provide 3 dB better

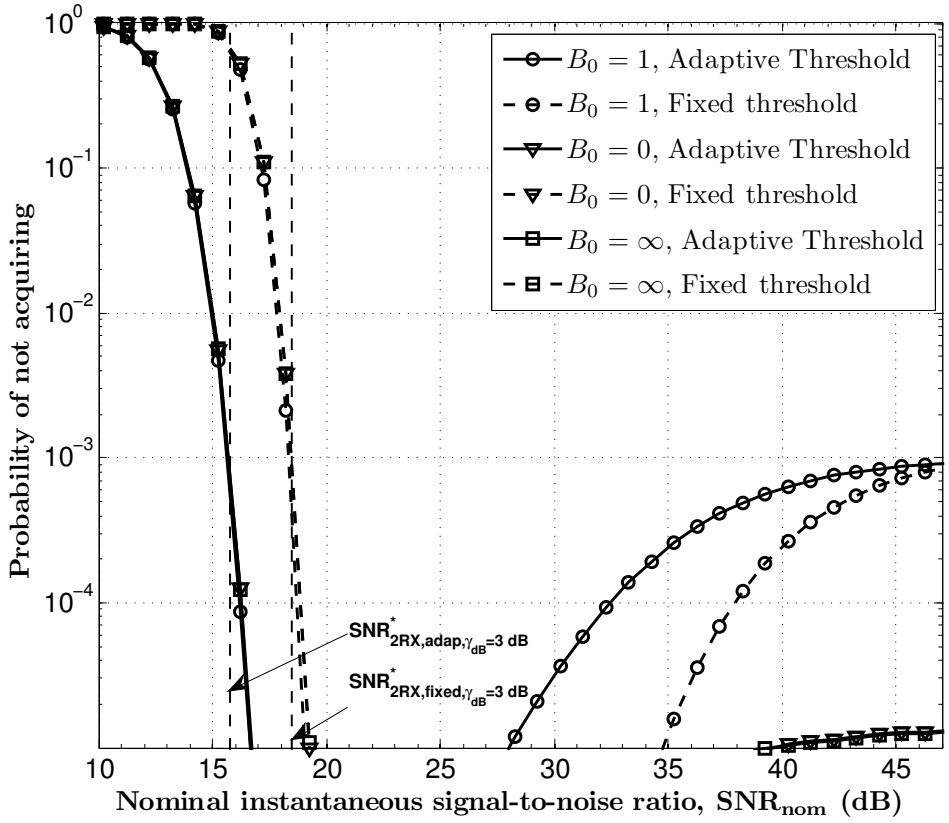

Figure 5.2: Acquisition performance of the single-transmitter, dual-receiver system in an AWGN channel with $\gamma_{dB} = 3$ dB.

performance than the dual-transmitting antenna diversity system, due to collection of signal energy at both receivers in the dual-receiver system. However, the actual gains using the dual-receiver system are observed to be significantly less than 3 dB. This is attributed to the correlation between the decision statistics in the two receiver chains, for the Q samples preceding the end of the arriving preamble.

The probability of not acquiring as a function of the signal-to-noise ratio is shown in Figs. 5.2 and 5.3 for the single-transmitter, dual-receiver example system considered above but with a noise factor degradation of $\gamma_{dB} = 3$ dB and $\gamma_{dB} = 20$ dB, respectively. The threshold parameters η and $\eta^{'}$ are equal to the respective thresholds optimized for

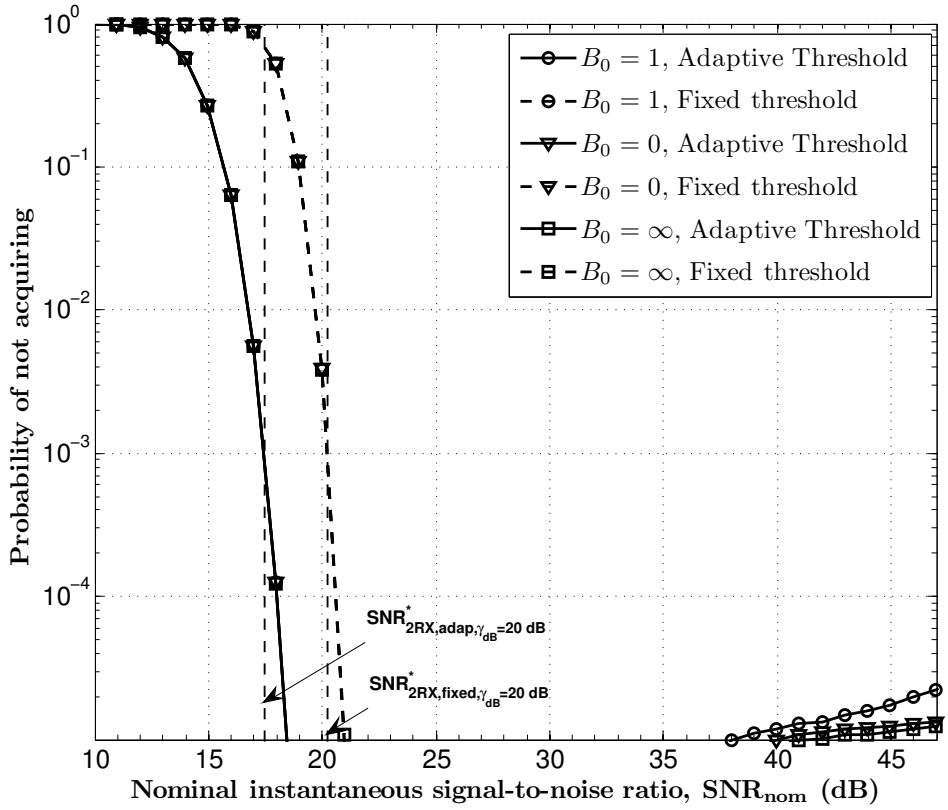

Figure 5.3: Acquisition performance of the single-transmitter, dual-receiver system in an AWGN channel with $\gamma_{dB} = 20$ dB.

$\gamma_{dB} = 0$ dB. From Figs. 5.2 and 5.3, it is observed that

$$SNR^*_{1TX2RX,fixed,\gamma_{dB}=3\text{ dB}} = 18.5 \text{ dB and } SNR^*_{1TX2RX,fixed,\gamma_{dB}=20\text{ dB}} = 20.2 \text{ dB}$$

using the fixed-threshold algorithm and

$$SNR^*_{1TX2RX,adap,\gamma_{dB}=3\text{ dB}} = 15.8 \text{ dB and} SNR^*_{1TX2RX,adap,\gamma_{dB}=20\text{ dB}} = 17.5 \text{ dB}$$

using the adaptive-threshold algorithm. This means that in a static AWGN channel with $\gamma_{dB} = 3$ dB and $\gamma_{dB} = 20$ dB the performance is degraded by approximately 1.3 dB and 3 dB, respectively, when compared to $\gamma_{dB} = 0$ dB, irrespective of the acquisition algorithm used.

5.3 Performance in a Time-varying Channel

The probability of outage in the single-transmitter, dual-receiver system is defined as

$$P_{outage} = \Pr\left(SNR < SNR^*\right). \tag{5.9}$$

The expressions for probability of outage in slow Rician fading is given in Appendix B. The performance is illustrated by considering the system used as an example in Section 5.2 and the optimal threshold for each acquisition algorithm.

The probability of outage for the single-transmitter, single-receiver system, the dual-transmitter, single-receiver system, and the single-transmitter, dual-receiver system (with $\gamma_{dB} = 0$ dB) in a Rayleigh-fading channel is shown in Fig. 5.4 as a function of $\overline{SNR}$ for each acquisition algorithm. For a single-transmitter, dual-receiver system, the adaptive-threshold algorithm results in approximately 2.6 dB better performance than the fixed-threshold algorithm. For example, for an target outage probability of 0.1, the fixed-threshold algorithm requires $\overline{SNR} = 22.8$ dB whereas the adaptive-threshold algorithm achieves the

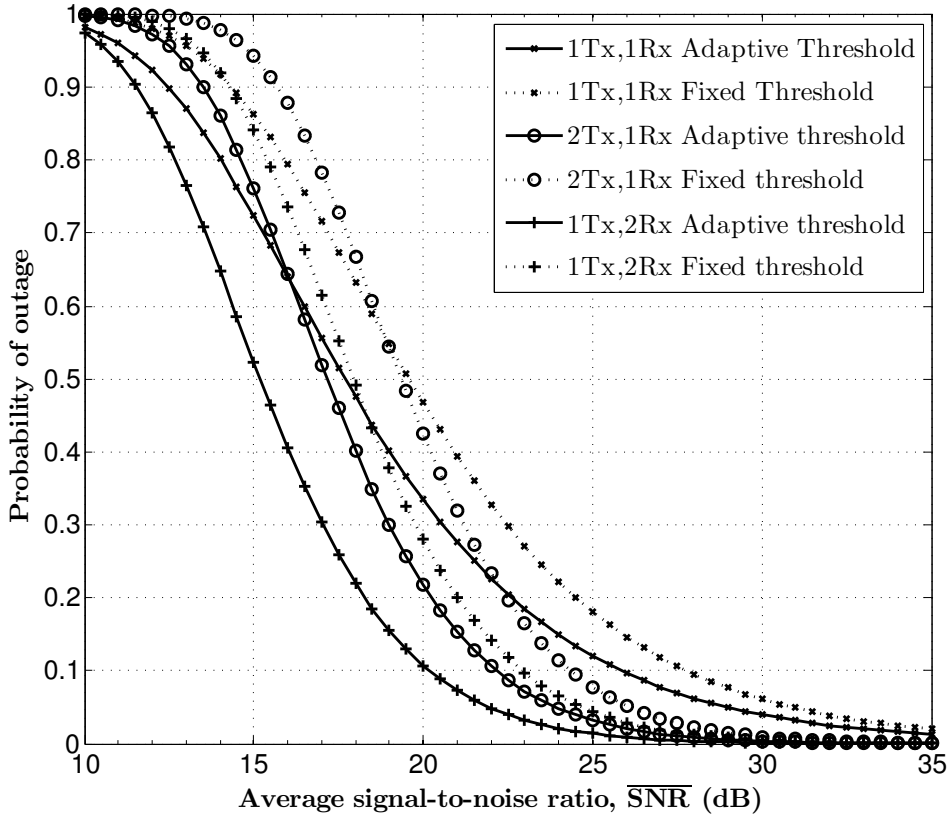

Figure 5.4: Outage probabilities for all three systems in a Rayleigh-fading channel.

same outage probability with $\overline{SNR} = 20.2$ dB. The corresponding values for the dual-transmitter, single-receiver system are $\overline{SNR} = 24.3$ dB with a fixed threshold and $\overline{SNR} = 22.1$ dB with an adaptive threshold. The values for the single-transmitter, single-receiver system are $\overline{SNR} = 27.7$ dB with a fixed threshold and $\overline{SNR} = 25.8$ dB with an adaptive threshold.

Thus, for a target outage probability of 0.1, the dual-receiver system is approximately 4.9 dB better than the single-transmitter, single-receiver system when fixed threshold is used. When adaptive threshold is used, the dual-receiver system is around 5.6 dB better than the single-transmitter, single-receiver system. Hence, it can be concluded that the dual diversity achieved with the two-receiver system results in more robustness against fading that more than offsets the receiver's non-coherent combining loss during acquisition, thus resulting in better performance than the single-transmitter system at outage probabilities of practical interest (i.e., low outage probabilities). The performance gap between the dual-receiver and the single-transmitter, single-receiver system expressed in decibels increases as a more stringent condition for the outage probability is imposed. At all outage probabilities, the dual receiving antenna diversity system is better than the dual transmitting antenna system by 1.5 dB if fixed threshold is used, and by 1.9 dB if adaptive threshold is used.

Suppose instead that the channel exhibits slow Rician fading with a specular-to-diffuse energy ratio of 12 dB. Once again, the adaptive-threshold algorithm provides 2.6 dB better performance than the fixed-threshold algorithm, regardless of the desired probability of outage. This is seen in Fig. 5.5. The difference in performance of the two-receiver system and the two-transmitter system is again independent of the outage probability and the two-receiver system is better again by 1.5 dB and 1.9 dB using the fixed-threshold algorithm and the adaptive-threshold algorithm, respectively. In contrast, the diversity benefits of the two-receiver system become less significant as the severity of channel fading decreases, and its performance advantage over the single-transmitter system diminishes accordingly. This is again shown in Fig. 5.5. The average signal-to-noise ratio required to achieve an

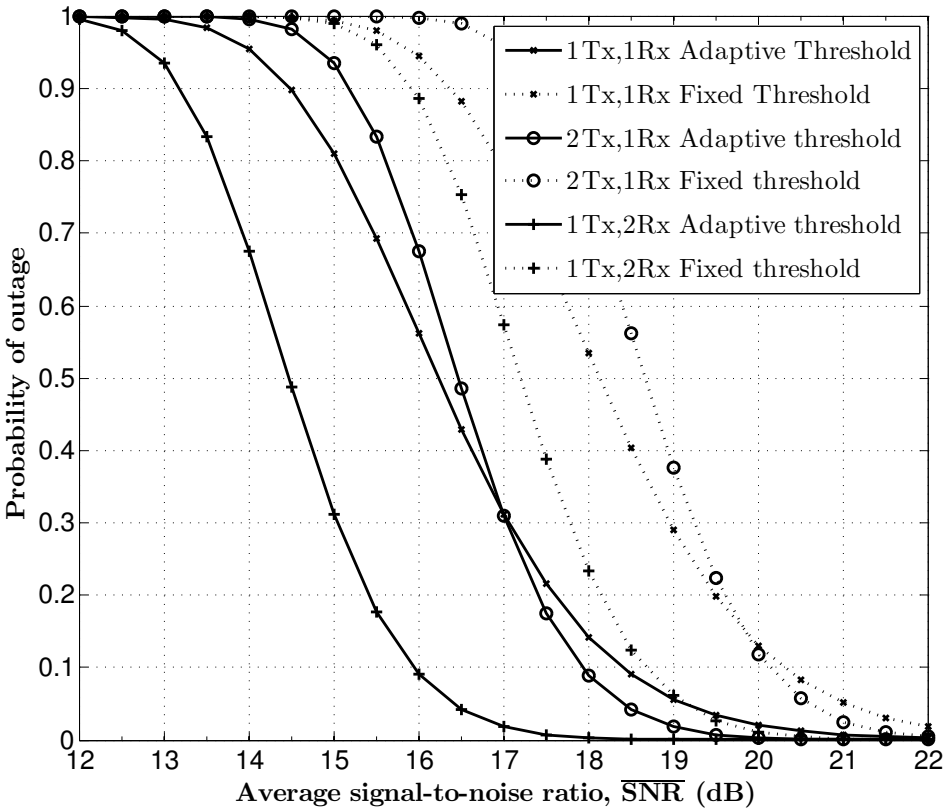

Figure 5.5: Outage probabilities for all three systems in a Rician-fading channel with a specular-to-diffuse energy ratio of 12 dB.

outage probability of 0.1 for the two-receiver system is only 2.5 dB lower than for the single-transmitter system if the adaptive-threshold algorithm is used and only 1.6 dB lower if a fixed threshold is used.

A further increase in the specular-to-diffuse energy ratio of the channel does not affect the difference in performance between the adaptive-threshold and fixed-threshold algorithms or the difference in performance between the dual-receiver and the dual-transmitter systems. In the limit, as the specular-to-diffuse energy ratio approaches infinity (i.e., as the channel approaches a constant-gain AWGN channel), the performance approaches that illustrated in Fig. 5.1, in which the single-transmitter, dual-receiver system performs better than the single-transmitter, single-receiver system by 0.9 dB if fixed threshold is used and by 1.6 dB if adaptive threshold is used.

5.4 Effect of the Noise Factor Degradation in a Time-Varying Channel

The probability of outage in a Rayleigh-fading channel plotted against the average nominal signal-to-noise ratio, $\overline{SNR}_{nom}$ for noise factor degradations $\gamma_{dB} = 0$ dB, $\gamma_{dB} = 3$ dB and $\gamma_{dB} = 20$ dB is shown in Fig. 5.6. The case $\gamma_{dB} = 0$ dB corresponds to equal noise power spectral densities in the RF front-end of the two receivers; $\gamma_{dB} = 3$ dB corresponds to one of the receivers with twice the noise power spectral density as the other receiver, and $\gamma_{dB} = 20$ dB corresponds to the case where one of the receivers has a hundred times the noise power spectral density as the other receiver. In practice, the cause of $\gamma_{dB} = 3$ dB scenario may be due to the inherent differences in the characteristics of the analog components, whereas the $\gamma_{dB} = 20$ dB scenario is more likely due to complete failure of one of the receiver chains.

From Fig. 5.6, for a dual-receiver system operating in a Rayleigh-fading channel, a noise factor degradation of 3 dB leads to a performance degradation of 1.5 dB using the fixed-threshold algorithm and 2.1 dB using the adaptive-threshold algorithm, irrespective

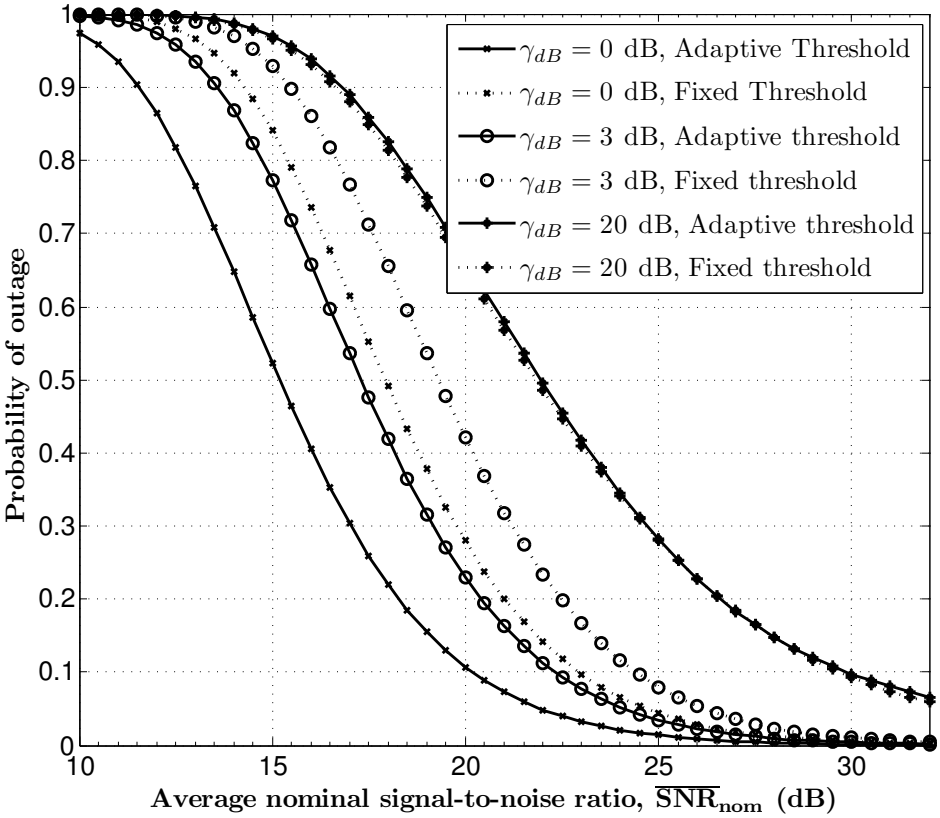

Figure 5.6: Effect of noise factor degradation on the outage probability of a dual-receiver system in a Rayleigh-fading channel.

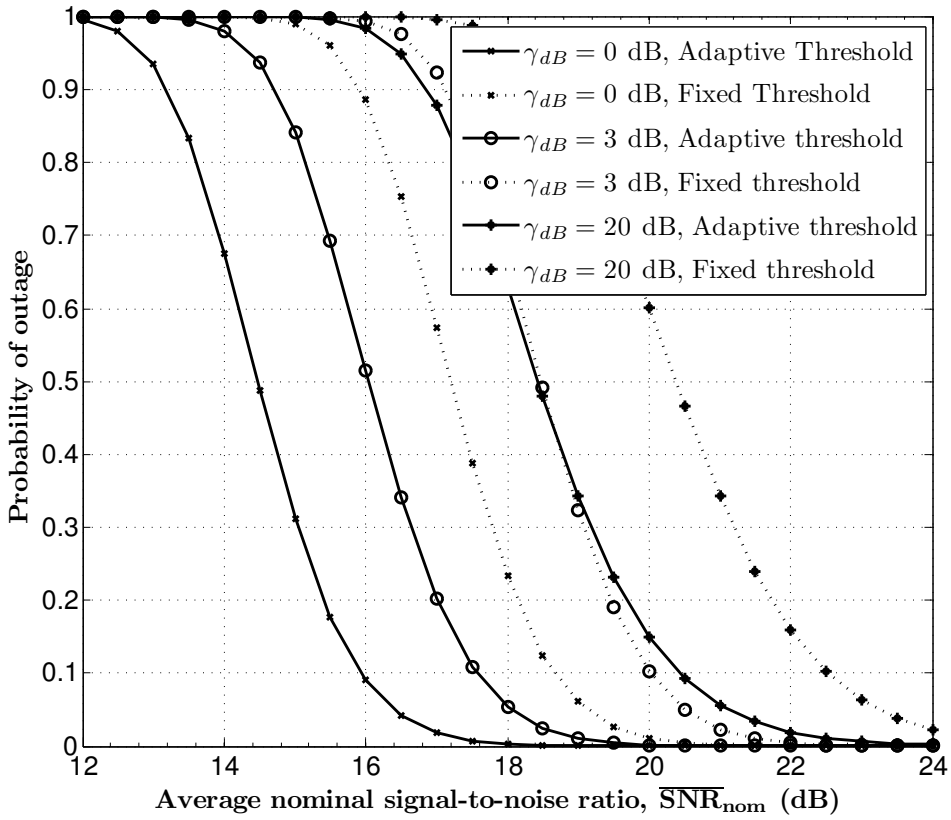

Figure 5.7: Effect of noise factor degradation on the outage probability of a dual-receiver system in a Rician-fading channel with a specular-to-diffuse energy ratio of 12 dB.

of the outage probability. The corresponding performance degradation values for a noise factor degradation of 20 dB is 6.8 dB using a fixed threshold and 9.6 dB using an adaptive threshold. Thus in a Rayleigh-fading channel, the adaptive threshold algorithm is more susceptible to the degradation in noise-power spectral density in the RF front-end of one of the receivers than the fixed-threshold algorithm.

As the specular-to-diffuse energy ratio of the channel increases (i.e., severity of fading decreases), we observe a significantly less performance degradation due to degradation of the noise power spectral density of one of the receivers, for both acquisition algorithms. This is shown in Fig. 5.7, for a dual-receiver system operating in a Rician-fading channel with a specular-to-diffuse energy ratio of 12 dB. A noise factor degradation of 3 dB leads to

a performance degradation of 1.3 dB using the fixed-threshold algorithm and 1.6 dB using the adaptive-threshold algorithm, irrespective of the outage probability. The performance degradation values for a noise factor degradation of 20 dB is dependent on the outage probability. At an outage probability of 0.1, the performance degradation values for a noise factor degradation of 20 dB are 3.8 dB using a fixed threshold and 4.5 dB using an adaptive threshold.

The adaptive-threshold algorithm is still more susceptible than the fixed-threshold algorithm to degradation in noise power spectral density of one of the receivers. However, as the specular to diffuse energy ratio increases, a degradation in the noise power spectral density of one of the receivers affects both the algorithms more and more equally. The performance degradation due to the two algorithms in the Rician-fading channel are less different (only 0.3 dB difference) as compared to a Rayleigh-fading channel (almost 0.6 dB difference). As the specular-to-diffuse energy ratio approaches infinity, the performance approaches that in an AWGN channel and there is equal performance degradation in both the acquisition algorithms due to a degradation in the noise power spectral density of one of the receivers.

Chapter 6

Conclusions and Discussion

Non coherent, serial, matched-filter packet acquisition using square-law combining is considered for a system with no antenna diversity, a system with dual transmitting antenna diversity and a system with dual receiving antenna diversity. Two acquisition algorithms are considered for all three systems: one using a fixed acquisition threshold, and the other using an adaptive acquisition threshold. The performance is evaluated and compared for the three systems using the two algorithms in both static and dynamic channels.

It is shown that in a static AWGN channel, using dual transmitting antenna diversity results in a few tenths of a decibel loss in acquisition performance compared with a system with no antenna diversity. This phenomenon is attributed to the non-coherent combining loss in forming the test statistics for the two-transmitter system. In dynamic channels susceptible to significant fading, however, the diversity gains provided by the two-transmitter system result in system outage performance that is over 3 dB better than the performance obtained with the single-transmitter system using the same acquisition algorithm, regardless of which algorithm is considered. The performance benefit decreases as the severity of fading decreases, and the system results in slightly poorer outage performance than the single-transmitter system due to the non-coherent combining loss if the channel exhibits negligible fading.

It is also shown that in static, equal-gain AWGN channels, the system with dual

receiving antennas achieves better acquisition performance than either of the single-receiver systems. The dual-receiver system recovers twice the signal energy of the dual-transmitter system; the 3 dB increase in received transmitted signal power is partially offset by the effect of correlation of the test statistics in the dual-receiver system's two receiver chains, however. The net result is that the dual-receiver system achieves approximately 1.5 dB better performance than the dual-transmitter system in equal-gain AWGN channels.

In dynamic channels with severe fading, the dual-receiver system is at least 5 dB better than the the single-transmitter, single-receiver system and at least 1.5 dB better than the dual-transmitter, single-receiver systems, irrespective of the acquisition algorithm used. As the severity of fading decreases, the performance benefit of the dual-receiver system over the single-transmitter, single-receiver system reduces. On the contrary, the performance benefit of the dual-receiver system over the dual-transmitter system remains constant, irrespective of the channel conditions.

The performance degradation due to different noise power spectral densities in the RF front-end of the two receiver chains was evaluated and quantified under different channel conditions. For all three acquisition systems considered, the adaptive-threshold acquisition algorithm provides around 2 dB (or a few-tenths of a decibel higher than 2 dB) improvement in performance over the fixed-threshold acquisition algorithm.

Appendices

Appendix A Spectral Decomposition of a Hermitian Quadratic Form in a Complex Gaussian Random Vector

In Chapter 5, the test statistic X_k, for $0 < k \leq M-1$ is the sum of the squared magnitudes of two complex-valued Gaussian random variables $Z_{0,k}$ and $Z_{1,k}$. Let the column vector with the elements $Z_{0,k}$, $Z_{1,k}$ be denoted by $\underline{Z_k}$. Let $\underline{Z_k}^H$ denoted the complex conjugate of the transpose of $\underline{Z_k}$. The decision statistic X_k for $0 < k \leq M-1$ can be represented as

$$X_k = \underline{Z_k}^H Q \underline{Z_k}$$

where $Q = I_2$, the two-by-two identity matrix. Since $Q^H = Q$, Q is a Hermitian matrix and X_k is a Hermitian quadratic form in the complex Gaussian random vector $\underline{Z_k}$ [12]. Generally it is hard to evaluate the distribution function of X_k directly, but X_k being a Hermitian Quadratic form in the complex Gaussian random vector $\underline{Z_k}$, the procedure to evaluate the distribution function of X_k can be simplified to a great extent as presented in [13]. A special case of this procedure relevant to our test statistic is presented below.

Assuming that $Z_{0,k}$ and $Z_{1,k}$ are jointly Gaussian, the mean and variance of $\underline{Z_k}$ are given by

$$\begin{aligned}
\underline{w_k} &= E[\underline{Z_k}] \\
&= [\ 0 \quad 0\ ]^T \\
\Sigma_k &= E[(\underline{Z_k} - \underline{w_k})(\underline{Z_k} - \underline{w_k})^H] \\
&= E[\underline{Z_k Z_k}^H] \\
&= E\begin{bmatrix} Z_{0,k}Z_{0,k}^* & Z_{0,k}Z_{1,k}^* \\ Z_{1,k}Z_{0,k}^* & Z_{1,k}Z_{1,k}^* \end{bmatrix} \\
&= \begin{bmatrix} \mathrm{Var}(Z_{0,k}) & \mathrm{Cov}(Z_{0,k}, Z_{1,k}) \\ \mathrm{Cov}(Z_{1,k}, Z_{0,k}) & \mathrm{Var}(Z_{1,k}) \end{bmatrix}
\end{aligned}$$

where the matrix elements are given by equations (5.3) and (5.4). Since Σ_k is a Hermitian

matrix, it can be spectrally decomposed as

$$\Sigma_k = U_1 \Lambda U_1^H$$

where Λ is a diagonal matrix with the eigen values of Σ_k as diagonal entries, and U_1 is a unitary matrix, whose column vectors are eigen vectors of Σ_k.

Eigen values of Σ_k are evaluated as follows.

$$\begin{aligned} \det(\Sigma_k - \lambda I_2) &= 0 \\ \Rightarrow \begin{vmatrix} \mathrm{Var}(Z_{0,k}) - \lambda & \mathrm{Cov}(Z_{0,k}, Z_{1,k}) \\ \mathrm{Cov}(Z_{1,k}, Z_{0,k}) & \mathrm{Var}(Z_{1,k}) - \lambda \end{vmatrix} &= 0. \end{aligned} \tag{1}$$

The roots of the quadratic in λ from equation (1) are given by

$$\lambda_1 = (\mathrm{Var}(Z_{0,k}) + \mathrm{Var}(Z_{1,k}) - \Delta)/2 \tag{2}$$

and

$$\lambda_2 = (\mathrm{Var}(Z_{0,k}) + \mathrm{Var}(Z_{1,k}) + \Delta)/2 \tag{3}$$

where

$$\Delta = \sqrt{(\mathrm{Var}(Z_{0,k}) - \mathrm{Var}(Z_{1,k}))^2 + 4|\mathrm{Cov}(Z_{0,k}, Z_{1,k})|^2}.$$

Eigen vectors of Σ_k or the column vectors of U_1 are found by solving for x, y in

$$(\Sigma_k - \lambda_l I_2)\underline{X} = 0 = (\Sigma_k - \lambda_2 I_2)\underline{X}$$

where $\underline{X} = [\ x \quad y\ ]^T$. The eigen vectors are

$$\underline{X_1} = c_1 \left[\ 1 \quad \frac{-2\mathrm{Cov}(Z_{0,k}, Z_{1,k})^*}{\Delta - (\mathrm{Var}(Z_{0,k}) - \mathrm{Var}(Z_{1,k}))}\ \right]^T$$

and

$$\underline{X_2} = c_2 \left[\begin{array}{cc} \frac{2\mathrm{Cov}(Z_{0,k},Z_{1,k})}{\Delta-(\mathrm{Var}(Z_{0,k})-\mathrm{Var}(Z_{1,k}))} & 1 \end{array} \right]^T$$

where c_1, c_2 are any real numbers. If $U_1 = [\ X_2 \quad X_1\ ]$, and if $c_1 = c_2 = c$, a real number then

$$U_1 = c \left[\begin{array}{cc} \frac{2\mathrm{Cov}(Z_{0,k},Z_{1,k})}{\Delta-(\mathrm{Var}(Z_{0,k})-\mathrm{Var}(Z_{1,k}))} & 1 \\ 1 & \frac{-2\mathrm{Cov}(Z_{0,k},Z_{1,k})^*}{\Delta-(\mathrm{Var}(Z_{0,k})-\mathrm{Var}(Z_{1,k}))} \end{array} \right]$$

where $c = \sqrt{(\Delta - (\mathrm{Var}(Z_{0,k}) - \mathrm{Var}(Z_{1,k})))/2\Delta}$ makes U_1 a unitary matrix. Also,

$$\Lambda = \left[\begin{array}{cc} \lambda_2 & 0 \\ 0 & \lambda_1 \end{array} \right].$$

Similarly, the matrix $\Lambda^{1/2} U_1^H Q U_1 \Lambda^{1/2}$ is also Hermitian and can be spectrally decomposed as

$$\Lambda^{1/2} U_1^H Q U_1 \Lambda^{1/2} = U_2 D U_2^H$$

where U_2 is unitary and D is diagonal with diagonal elements $\{d_1, d_2\}$. $\Lambda^{1/2} U_1^H Q U_1 \Lambda^{1/2} = \Lambda$, and therefore $U_2 = I_2$, the 2 x 2 identity matrix and $D = \Lambda$. Suppose $\tilde{D}$ is a diagonal matrix with diagonal elements $\{|d_1|, |d_2|\}$. If we define the matrix $P = U_1 \Lambda^{1/2} U_2$, then the vector of uncorrelated chi-square random variables is given by

$$\underline{Y_k} = \tilde{D}^{1/2} P^{-1} \underline{Z_k}.$$

It can be proved using equations (2) and (3) that $\lambda_2 \geq \lambda_1 \geq 0$. Therefore $|d_l| = d_l$ for $l = 0, 1$. Hence $\tilde{D} = D = \Lambda$. Also $P = U_1 \Lambda^{1/2} U_2 = U_1 \Lambda^{1/2}$. Therefore,

$$\underline{Y_k} = U_1^H \underline{Z_k}$$

where $\underline{Y_k} = [\ Y_{0,k} \quad Y_{1,k}\ ]^T$. The test statistic can now be represented as

$$X_k = |Y_{0,k}|^2 + |Y_{1,k}|^2.$$

The complex-valued Gaussian random variables $Y_{0,k}$ and $Y_{1,k}$ are independent with mean and variance of the vector $\underline{Y_k}$ is given by

$$\begin{aligned} E[\underline{Y_k}] &= \tilde{D}^{1/2} P^{-1} \underline{w_k} \\ &= 0 \end{aligned}$$

and

$$\begin{aligned} E\left[(\underline{Y_k} - E[\underline{Y_k}])(\underline{Y_k} - E[\underline{Y_k}])^T\right] &= \Lambda \\ \Rightarrow \mathrm{Var}(Y_{0,k}) &= \lambda_2 \\ \text{and } \mathrm{Var}(\mathrm{Y_{1,k}}) &= \lambda_1. \end{aligned}$$

Appendix B Probability of Outage in Slow Rician Fading

B.1 Single-Transmitter, Single-Receiver System

Consider the single-transmitter, single-receiver system using either fixed-threshold acquisition or adaptive-threshold acquisition and the optimal threshold parameter for the corresponding algorithm and the system. From equations (3.6) and (2.2.1), the probability of outage is given by

$$\begin{aligned} P_{outage} &= \Pr\left(A^2 \frac{MPT_C}{N_0} < SNR^*\right) \\ &= \Pr\left(A^2 < \frac{N_0 SNR^*}{MPT_c}\right) \\ &= \Pr\left(S < \frac{N_0 SNR^*}{MPT_c}\right) \end{aligned}$$

where $S = A^2$ and SNR^* is defined in Section 3.2. The random variable $S = A^2$ follows a chi-square distribution with two degrees of freedom [7] with

$$\mathrm{E}[A] = \mu \ \text{ and } \ \mathrm{Var}(A) = 2\sigma^2.$$

The outage probability is thus given by

$$\begin{aligned} P_{outage} &= F_S(c) \\ &= \begin{cases} 1 - e^{-c/2\sigma^2}, & \mu = 0 \\ 1 - Q_1\left(\frac{\mu}{\sigma}, \frac{\sqrt{c}}{\sigma}\right), & \mu \neq 0 \end{cases}, \end{aligned} \tag{4}$$

where $c = \frac{N_0 SNR^*}{MPT_c}$ and $Q_m(a, b)$ is the generalized Marcum Q-function [7].

From equation (2.1), the average signal-to-noise ratio of the channel is given by

$$\overline{SNR} = 2\sigma^2(1 + SDER)\frac{MPT_c}{N_0} \tag{5}$$

where

$$SDER = \mu^2/2\sigma^2 \tag{6}$$

is the specular-to-diffuse energy ratio of the Rician-fading channel. Thus,

$$\frac{\mu^2}{\sigma^2} = 2\ SDER,$$
$$\frac{c}{\sigma^2} = \frac{2(1+SDER)SNR^*}{\overline{SNR}}.$$

It follows from equation (4) that the outage probability for the single-transmitter, single-receiver system using an acquisition algorithm corresponding to SNR^* is

$$P_{outage} = \begin{cases} 1 - e^{-SNR^*/\ \overline{SNR}}, & SDER = 0 \\ 1 - Q_1\left(\sqrt{2\ SDER}, \sqrt{\frac{2(1+SDER)SNR^*}{\overline{SNR}}}\right), & SDER \neq 0 \end{cases}.$$

B.2 Dual-Transmitter, Single-Receiver System

From equations (3.6) and (2.2), the probability of outage for the acquisition system using two transmitting antennas and a single receiving antenna is given by

$$\begin{aligned} P_{outage} &= \Pr\left(\left(\frac{A_0^2 + A_1^2}{2}\right)\frac{MPT_C}{N_0} < SNR^*\right) \\ &= \Pr\left(A_0^2 + A_1^2 < \frac{2N_0 SNR^*}{MPT_c}\right) \\ &= \Pr\left(S < \frac{2N_0 SNR^*}{MPT_c}\right) \end{aligned}$$

where $S = A_0^2 + A_1^2$ and SNR^* is again as defined in Section 3.2. For independent Rician-fading channels, $S = A_0^2 + A_1^2$ is a chi-square random variable with four degrees of freedom [7] and

$$\mathrm{E}[A_l] = \mu \ \text{ and } \ \mathrm{Var}(A_l) = 2\sigma^2\ ,\ 0 \leq l \leq 1.$$

The outage probability is thus given by

$$\begin{aligned} P_{outage} &= F_S(c_1) \\ &= \begin{cases} 1 - e^{-c_1/2\sigma^2} - \frac{c_1}{2\sigma^2} e^{-c_1/2\sigma^2}, & \mu = 0 \\ 1 - Q_2\left(\frac{\sqrt{2}\mu}{\sigma}, \frac{\sqrt{c_1}}{\sigma}\right), & \mu \neq 0 \end{cases}, \end{aligned} \tag{7}$$

where $c_1 = \frac{2N_0 SNR^*}{MPT_c}$ and $Q_m(a, b)$ is the generalized Marcum Q-function [7].

From equation (2.1), the average received signal-to-noise ratio and the specular-to-diffuse energy ratio of the Rician-fading channels are given by equations (5) and (6), respectively. Thus,

$$\begin{aligned} \frac{\mu^2}{\sigma^2} &= 2\ SDER, \\ \frac{c_1}{\sigma^2} &= \frac{4(1 + SDER)SNR^*}{\overline{SNR}}. \end{aligned}$$

It follows from equation (7) that the outage probability for the dual-transmitter, single-receiver system using an acquisition algorithm corresponding to SNR^* is

$$P_{outage} = \begin{cases} 1 - e^{-2\ SNR^*/\ \overline{SNR}} - \frac{2SNR^*}{\overline{SNR}} e^{-2\ SNR^*/\ \overline{SNR}}, & SDER = 0 \\ 1 - Q_2\left(\sqrt{4\ SDER}, \sqrt{\frac{4(1+SDER)SNR^*}{\overline{SNR}}}\right), & SDER \neq 0 \end{cases}.$$

B.3 Single-Transmitter, Dual-Receiver System

From equations (5.9) and (2.3), the probability of outage for the dual-receiver system is

$$\begin{aligned} P_{outage} &= \Pr\left(\frac{1}{2}\left(A_0^2 + \frac{N_0}{N_1}A_1^2\right)\frac{MPT_C}{N_0} < SNR^*\right) \\ &= \Pr\left(A_0^2 + \frac{N_0}{N_1}A_1^2 < \frac{2N_0 SNR^*}{MPT_c}\right) \\ &= \Pr\left(S_0 + S_1 < \frac{2N_0 SNR^*}{MPT_c}\right) \end{aligned}$$

where $S_0 = A_0^2$ and $S_1 = (N_0/N_1)A_1^2$ are independent chi-square random variables with parameters (μ_0, σ_0^2) and (μ_1, σ_1^2) respectively and SNR^* is defined in Section 5.2. The parameters are given by

$$\mu_0^2 = \mu^2, \sigma_0^2 = \sigma^2, \mu_1^2 = \gamma^{-1}\mu^2, \sigma_1^2 = \gamma^{-1}\sigma^2$$

For independent Rician-fading channels, $S = S_0 + S_1$ is the sum of two independent chi-square random variables with two degrees of freedom [7] and

$$\mathrm{E}[A_l] = \mu \text{ and } \mathrm{Var}(A_l) = 2\sigma^2 \ , \ 0 \leq l \leq 1.$$

The outage probability is thus given by

$$P_{outage} = F_S(c_1) \tag{8}$$

where $c_1 = \frac{2N_0 SNR^*}{MPT_c}$. In i.i.d. Rayleigh-fading channels, the distribution function for the sum of two uncorrelated central chi-square random variables with two degrees of freedom is given by

$$F_S(x) = \begin{cases} \frac{\sigma_0^2 F_{S_0}(x) - \sigma_1^2 F_{S_1}(x)}{\sigma_0^2 - \sigma_1^2}, & N_0 \neq N_1 \\ 1 - e^{-x/2\sigma_0^2} - \frac{x}{2\sigma_0^2} e^{-x/2\sigma_0^2}, & N_0 = N_1 \end{cases} \tag{9}$$

where $F_{S_l}(x) = 1 - e^{-x/2\sigma_l^2}$ for $l = 0, 1$ is the distribution of a central chi-square random variable with two degrees of freedom.

In i.i.d. Rician-fading channels, the distribution function for the sum of two uncorrelated non-central chi-square random variables with two degrees of freedom is given by

$$F_S(x) = \begin{cases} \int_0^x F_{S_0}(x-y) f_{S_1}(y) dy, & N_0 \neq N_1 \\ 1 - Q_2\left(\frac{\sqrt{2}\mu}{\sigma_0}, \frac{\sqrt{x}}{\sigma_0}\right), & N_0 = N_1 \end{cases} \tag{10}$$

where

$$F_{S_0}(x) = 1 - Q_1\left(\frac{\mu_0}{\sigma_0}, \frac{\sqrt{x}}{\sigma_0}\right),$$

$$f_{S_1}(x) = \frac{1}{2\sigma_1^2} e^{-\frac{\mu_1^2+x}{2\sigma_1^2}} I_0\left(\frac{\sqrt{x}\mu_1}{\sigma_1^2}\right),$$

$Q_m(a,b)$ is the generalized Marcum Q-function and $I_n(z)$ is the n^{th} order modified Bessel function of the first kind [7].

From equation (2.4), the average received signal-to-noise ratio is given by

$$\overline{SNR} = 2\sigma^2(1 + SDER)\left(\frac{1+\gamma^{-1}}{2}\right)\frac{MPT_c}{N_0}$$

where $SDER$ is given by equation (6). Thus,

$$\frac{\mu^2}{\sigma^2} = \frac{\mu_0^2}{\sigma_0^2} = \frac{\mu_1^2}{\sigma_1^2} = 2\ SDER,$$

$$\frac{c_1}{\sigma_0^2} = \frac{2(1+SDER)(1+\gamma^{-1})SNR^*}{\overline{SNR}}$$

and

$$\frac{c_1}{\sigma_1^2} = \gamma\frac{c_1}{\sigma_0^2}.$$

It follows from equations (8),(9) and (10) that the outage probability for the single-transmitter, dual-receiver system using an acquisition algorithm corresponding to SNR^* is

$$P_{outage} = \begin{cases} 1 - \left(\frac{e^{-\epsilon} - \gamma^{-1}e^{-\gamma\epsilon}}{1-\gamma^{-1}}\right), & \gamma \neq 1,\ SDER = 0 \\ 1 - e^{-\epsilon} - \epsilon e^{-\epsilon}, & \gamma = 1,\ SDER = 0 \\ \int_0^{\gamma\epsilon}(1 - Q_1(\sqrt{2\ SDER}, \sqrt{2\epsilon - 2\gamma^{-1}u})) & \\ \quad e^{-(SDER+u)}I_0(\sqrt{4\ u\ SDER})du, & \gamma \neq 1,\ SDER \neq 0 \\ 1 - Q_2\left(\sqrt{4\ SDER}, \sqrt{2\epsilon}\right), & \gamma = 1,\ SDER \neq 0 \end{cases}$$

where $\epsilon = \frac{(1+SDER)(1+\gamma^{-1})SNR^*}{\overline{SNR}}$.

Bibliography

[1] D. L. Noneaker, "The performance of serial, matched-filter acquisition in direct-sequence packet radio communications," in *Proceedings of the IEEE Military Communications Conference*, vol. 2, McLean, VA, Oct 2001, pp. 1045–1049.

[2] A. Polydoros and C. L. Weber, "A unified approach to serial search spread-spectrum code acquisition-part II : A matched-filter receiver," *IEEE Transactions on Communications*, vol. 32, no. 5, pp. 550–560, May 1984.

[3] D. L. Noneaker, A. R. Raghavan, and C. W. Baum, "The effect of automatic gain control on serial, matched-filter acquisition in direct-sequence packet radio communications," *IEEE Transactions on Vehicular Technology*, vol. 50, no. 4, pp. 1140–1150, July 2001.

[4] A. Swaminathan and D. L. Noneaker, "A technique to improve the performance of serial, matched-filter acquisition in direct-sequence spread-spectrum packet radio communications," *IEEE Journal on Selected Areas in Communications*, vol. 23, no. 5, pp. 909–919, May 2005.

[5] S. M. Alamouti, "A simple transmit diversity technique for wireless communications," *IEEE Journal on Selected Areas in Communications*, vol. 16, no. 8, pp. 1451–1458, Oct 1998.

[6] D. G. Brennan, "Linear diversity combining techniques," *Proceedings of the IRE*, vol. 47, no. 6, pp. 1075–1102, June 1959.

[7] J. G. Proakis, *Digital Communications*, 4th ed. New York: McGraw-Hill, 2000.

[8] B. Razavi, *RF Microelectronics*. Upper Saddle River, NJ: Prentice-Hall, 1998.

[9] D. V. Sarwate and M. B. Pursley, "Crosscorrelation properties of pseudorandom and related sequences," *Proceedings of the IEEE*, vol. 68, no. 5, pp. 593–619, May 1980.

[10] F. D. Neeser and J. L. Massey, "Proper complex random processes with applications to information theory," *IEEE Transactions on Information Theory*, vol. 39, no. 4, pp. 1293–1302, July 1993.

[11] M. Schwartz, W. R. Bennett, and S. Stein, *Communication Systems and Techniques*. New York: McGraw-Hill, 1966.

[12] G. L. Turin, "The characteristic function of Hermitian quadratic forms in complex normal variables," *Biometrika*, vol. 47, no. 1/2, pp. 199–201, June 1960.

[13] D. L. Noneaker, "The performance of direct-sequence spread-spectrum communications with selective fading channels and rake reception," Ph.D. dissertation, University of Illinois at Urbana-Champaign, 1993.